BULLETIN OF THE EARTHQUAKE
RESEARCH INSTITUTE
UNIVERSITY OF TOKYO
Vol. 64 (1989), pp. 1-36

Heat Flow in Central Japan and its Relations to Geological and Geophysical Features

Xinyuan LI[1] Yoshitsugu FURUKAWA[1] Toshiyasu NAGAO[1]*
Seiya UYEDA[1] and Hiroyoshi SUZUKI[2]

[1] Earthquake Research Institute
[2] National Research Center for Disaster Prevention

(Received December, 1988)

Abstract

An investigation on the distribution of surface heat flow in central Japan was carried out using bore-holes of the Kanto-Tokai seismic network of the National Research Center for Disaster Prevention, and holes drilled for geological survey by the Water Resources Development Public Cooperation, the Kanto Regional Construction Bureau and the Chubu Regional Construction Bureau. Topographic effects on heat flow values measured in areas of high topographic variation were taken into account. Eighteen new heat flow values were obtained and three additional data were provided by NEDO (the New Energy Development Organization).

On the basis of the new data combined with previous data, a heat flow contour map of the area was prepared, delineating a very broad zone of low heat flow through the central to eastern part of the Kanto district and a low heat flow zone in the western part of the Tokai district. Heat flow increases up to over 100 mw/m^2 towards the volcanic front. The low heat flow in these two areas can be interpreted as the cooling effect of subduction of the Pacific Plate and the Philippine Sea Plate.

The temperature at the Moho discontinuity and mantle heat flow were estimated by a one-dimensional steady-state conductive model with two layers of granitic and basaltic composition. Mantle heat flow demonstrated a similar distribution to that of the surface heat flow.

A comparision was made between the features of the distribution of surface heat flow and those of variations of certain other geophysical characteristics. It was found that the surface heat flow correlates fairly well with the Curie isotherm, the attenuation structure in the layer of 30-60 km depth (HASHIDA, 1987), and seismicity at depths of 40-60 km.

* Now at the Faculty of Earth Science, Kanazawa University

1. Introduction

The first measurement of heat flow in Japan was made in 1957. During the next two decades more than 500 heat flow values were obtained in and around Japan (HORAI and UYEDA, 1964; UYEDA, 1972; HONDA *et al.*, 1979). WATANABE *et al.* (1977) compiled the western Pacific heat flow data, recognizing a characteristic pattern of heat flow in the subduction zone, that is, low heat flow in trenches, anomalously high heat flow in volcanic arcs, and relatively high heat flow in back-arc basins. In recent years, more heat flow data were added both on land and at sea, and thermal structure and thermal processes of the subduction zone have also been discussed (HONDA and UYEDA, 1984; FURUKAWA and UYEDA, 1986).

However, there were few heat flow data available in central Japan compared with other regions in Japan, though it is very important in understanding arc evolution and origin of volcanism. Previous studies in this area include 16 data in Hokuriku, the northwestern part of central Japan, reported by KONO and KOBAYASHI (1971), and 12 measurements made from metal mine tunnels or other available bore-holes (UYEDA and HORAI, 1963).

To clarify the thermal state in this region, we carried out heat flow measurements in bore-holes of the Kanto-Tokai seismic network of the National Research Center for Disaster Prevention (NRCDP) and those of the Water Resources Development Public Cooperation (WRDPC), the Kanto Regional Construction Bureau (KRCB) and The Chubu Regional Construction Bureau (CRCB) for geological survey. Also, correlations between the distribution of heat flow and other geological and geophysical observations in the same region were examined.

2. Geological and Geophysical Background

Fig. 1 illustrates geological structures in central Japan. The main geologic terrains of central Japan bend sharply forming a cusp at the Fossa Magna, central Honshu, where the Izu-Bonin arc joins with it. Highly compressive deformation, strong Quaternary uplift and anomalous trajectories of crustal stress axis also characterize the South Fossa Magna region. These features can be described within the framework of plate tectonics as belonging to a boundary area of three plates: Pacific, Philippine Sea and Eurasia (MATSUDA, 1978; NAKAMURA *et al.*, 1983; NIITSUMA and MATSUDA, 1985).

As shown in Fig. 1, the pre-Miocene terrains were generally divided

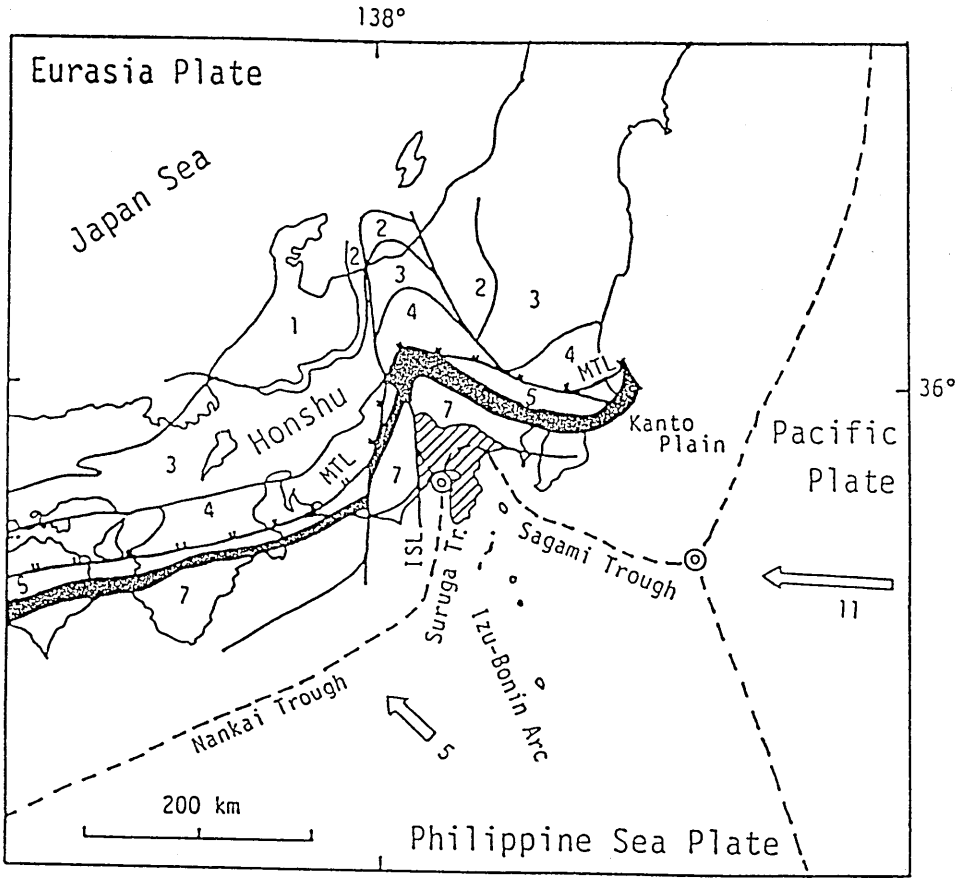

Fig. 1. The geological setting in the studied area and its surroundings (after Niitsuma and Matsuda, 1985). 1: Hida Belt, 2: Hida Marginal-Joetsu Belt, 3: Mino-Tamba-Ashio Belt, 4: Ryoke Belt, 5: Sambagawa Belt, 6: Chichibu and Sambosan Belts (black), 7: Shimanto Belt, MTL: Median Tectonic Line, ISL: Itogiwa-Shizuoka Tectonic Line, arrow: direction of present relative plate motion.

into nine belts according to NIITSUMA and MATSUDA (1985). These are the Hida, Hida marginal-Joetsu, Mino-Tamba-Ashio, Ryoke, Sambagawa, Mikabu, Chichibu, Sambosan, and Shimanto belts from north to south. These zonal structures and two great tectonic lines, the Itoigawa-Shizuoka Tectonic Line and the Median Tectonic Line, dominate the geotectonic evolution of the region.

Many active volcanoes associated with the west-dipping subduction of the Pacific plate and the collision of the Philippine Sea plate with the Honshu Island are distributed along the volcanic front. The composition of those volcanoes is mainly basaltic and andesitic. Miocene

volcanism is another activity found in the south Fossa Magna region. This activity is related to subduction of the Pacific plate (NIITSUMA and MATSUDA, 1985). These volcanic activities may contribute greatly to the geothermal structure in this region.

Geophysical observations have been extensively carried out in this region in recent years, including seismicity, gravity, explosion seismology and magnetism. These observation data allow us to compare them with our heat flow data.

3. Data Acxuisition and Topographic Correction

3.1 Temperature measurement method

All temperature measurements were made using a conventional portable system consisting of a thermistor probe sensor, a resistance meter and two wire connecting cables. Takara A-820 type thermometers were used as temperature transducers, which can measure temperature from 0 to 200°C with a resolution of 0.01°C. Calibration of the thermometer system was made using a Yoshida Kagaku Kiki model 101 cryostat and a Hewlett Packard 2804A quartz thermometer

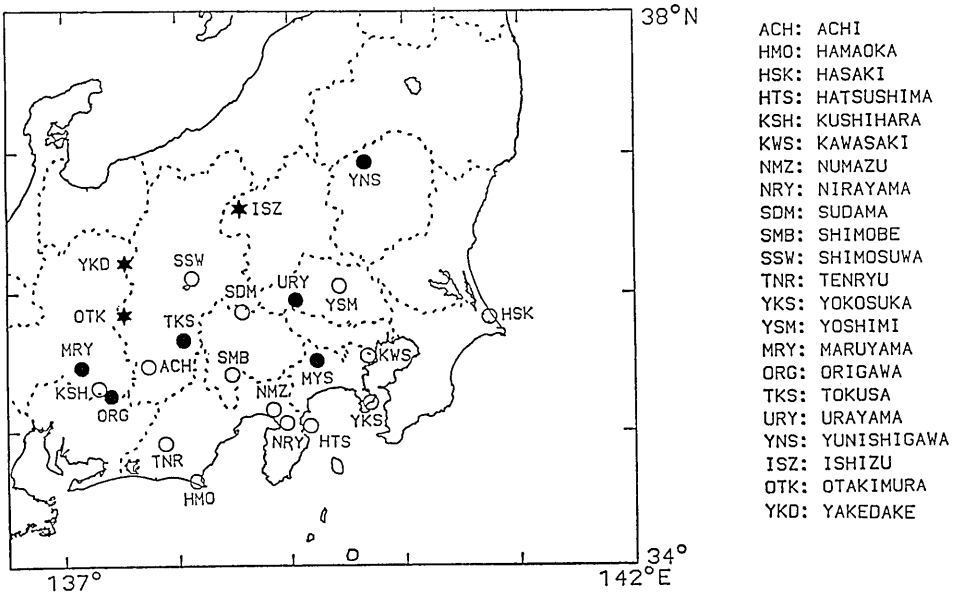

Fig. 2. Location map of heat flow measurements in this study. The star indicates the site of data provided by NEDO. The solid circle represents the location of holes for the Kanto and Chubu Regional Bureaus, and the Water Resources development Public Cooperation. The hollow circle denotes the site of holes for the National Research Center for Disaster Prevention.

at the Earthquake Research Institute, University of Tokyo.

Temperature was measured at fourteen boreholes of NRCDP drilled for seismic observation and five sites for geological survey by WRDPC, KRCB and CRCB in the Kanto and Tokai areas. Locations of these holes, including sites of the data obtained by the New Energy Development Organization (NEDO), are shown in Fig. 2.

3.2 Thermal conductivity measurement

Thermal conductivity measurement was carried out on samples collected from nearby outcrops based on geological column with QTM (Quick Thermal Conductivity Meter, see SASS *et al.*, 1984). The samples were saturated with water in order to reproduce the natural water-saturated condition. A standard glass plate with thermal conductivity of 1.15 W/mK was used for calibration. Reproducibility of measurement was within ±5%. For one site, 3-10 specimens were measured and their mean value was taken as representative for that site.

For the sites where no samples were available, we used the representative values of the equivalent kind of rocks to those in sites from the published data (CERMAK and RYBACH, 1982).

Results of thermal conductivity measurements in this study are listed in Table 1.

Table 1. Results of conductivity measurements

Locality	Number of samples	Mean value W/mK	Standard deviation
ACHI	11	3.14	0.183
HAMAOKA	3	1.21	0.047
HATSUSHIMA	10	1.64	0.149
KUSHIHARA	4	3.27	0.250
SHIMOBE	4	2.17	0.237
SHIMOSUWA	7	3.08	0.195
SUDAMA	2	2.36	0.083
TENRYU	6	3.93	0.334
YOKOSUKA	11	1.20	0.028
YOSHIMI	11	2.78	0.479

3.3 Description of observation sites of NRDPC

(1) Hamaoka

The drill-hole is located near the Cape Omaezaki. Rock type in this area is Miocene siltstone and mudstone covered with Quaternary sediments.

Temperatures were measured in the 100 m vertical drill-hole, drilled through alternating layers of mudstone and siltstone. The measurement was carried out on June 20, 1987. The measured temperature-

depth profile from the bore-hole is plotted in Fig. 3-A.

(2) Achi

This site is located in the Ryoke metamorphic belt, only 16 km from the Median Tectonic Line, one of the biggest tectonic lines in Japan. The area is composed of granite and hornfels.

The drill-hole which is 113 m in vertical depth penetrates mainly biotite granodiorite and hornfels. The measurement was made on July 2, 1987. The temperature-depth profile is presented in Fig. 3-B.

(3) Numazu

The observation point is located at the southeast foot of the Ashitaka volcano. Tuff, andesitic lava and volcanic sandstone are the predominant rock types in the locality.

The 100 m vertical drill-hole penetrates tuff and tuff-sandstone underlain by about 10 m of andesitic lava in the bottom part. Temperatures were logged on June 19, 1987. The temperature-depth profile is shown in Fig. 3-C.

(4) Kushihara

This site is situated at the northwest side of the Median Tectonic Line. and it belongs to the Ryoke belt. The area is made up of the Ryoke metamorphic rocks and late Cretaceous intrusive granite.

The hole was drilled in the granite layer. This granite is classified to be of granodiorite type. Temperature determination was made to the vertical depth of 100 m on July 3, 1987, and the result is illustated in Fig. 3-D.

(5) Nirayama

The site is located in the neck of Izu Peninsula, which consists mainly of Quaternary volcanoes. The Tanna fault runs through the central part of the area. A few basins are distributed along the fault.

The drill-hole is 110 m in vertical depth. Most of the rocks in the hole are andesitic lava, with some intercalation of tuff. Fig. 4-A shows the result of the temperature measurement which was made on June 20, 1987.

(6) Hatsushima

This is a small volcanic island located to the east of Izu Peninsula. The rocks consist mainly of basaltic lava, tuff and lapilli tuff.

The hole is on the slope gently inclining to the north. The dominant lithology in the hole is basaltic lava intercalated with thin tuff layers. Temperatures were determined to the depth of 70 m on May 20, 1987. Fig. 4-B shows the temperature-depth profile. In this hole, the temperature gradient changes at the depth of 40 m. This may be due to the circulation of water of thermal origin. We only used the temperature data between the interval of 40 and 70 m.

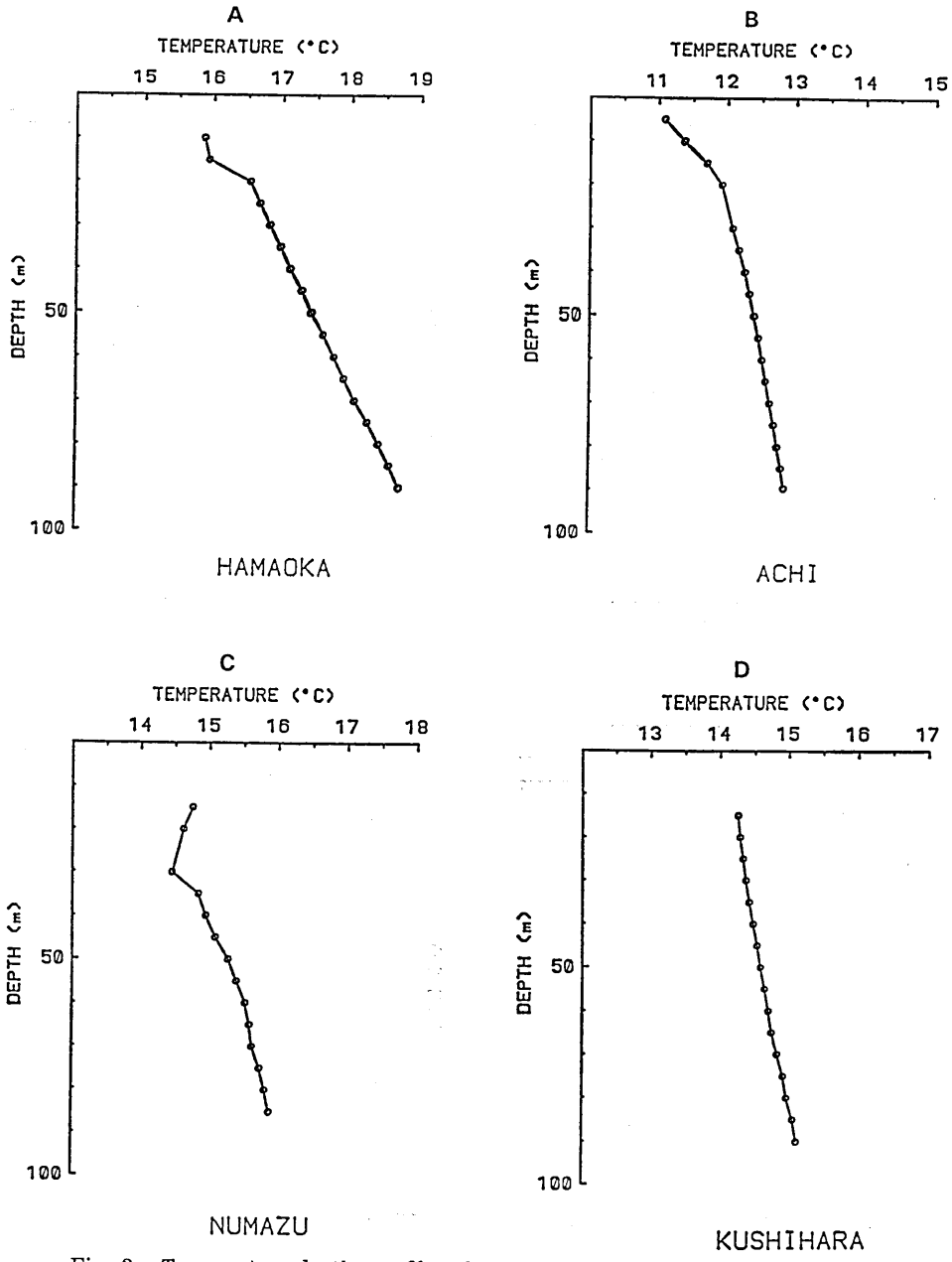

Fig. 3. Temperature-depth profiles for the drill-holes of the Kanto-Tokai seismic network of the National Research Center for Disaster Prevention. A) HAMAOKA; B) ACHI; C) NUMAZU; D) KUSHIHARA.

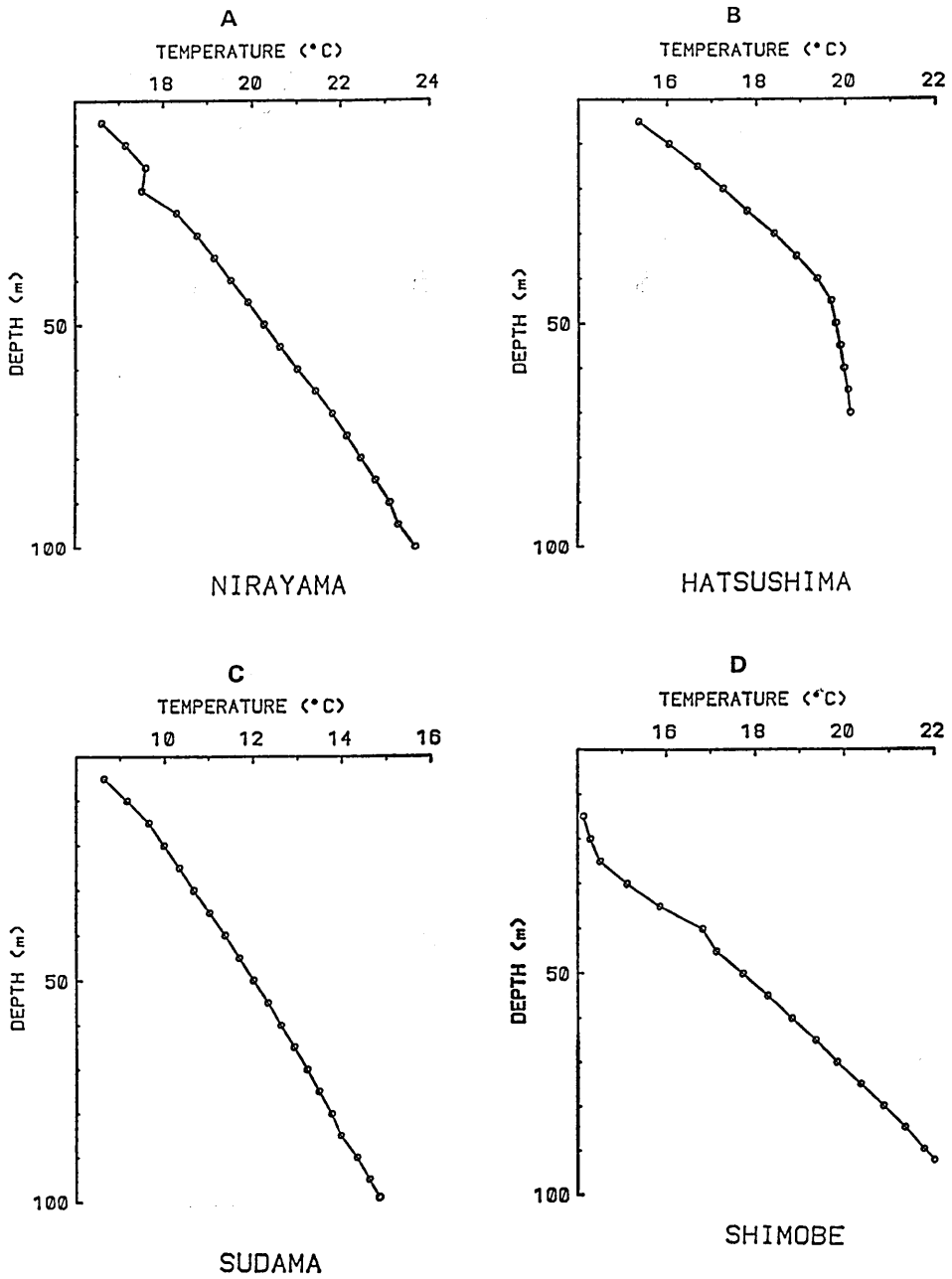

Fig. 4. The results of temperature measurements. A) NIRAYAMA; B) HATSUSHIMA; C) SUDAMA; D) SHIMOBE.

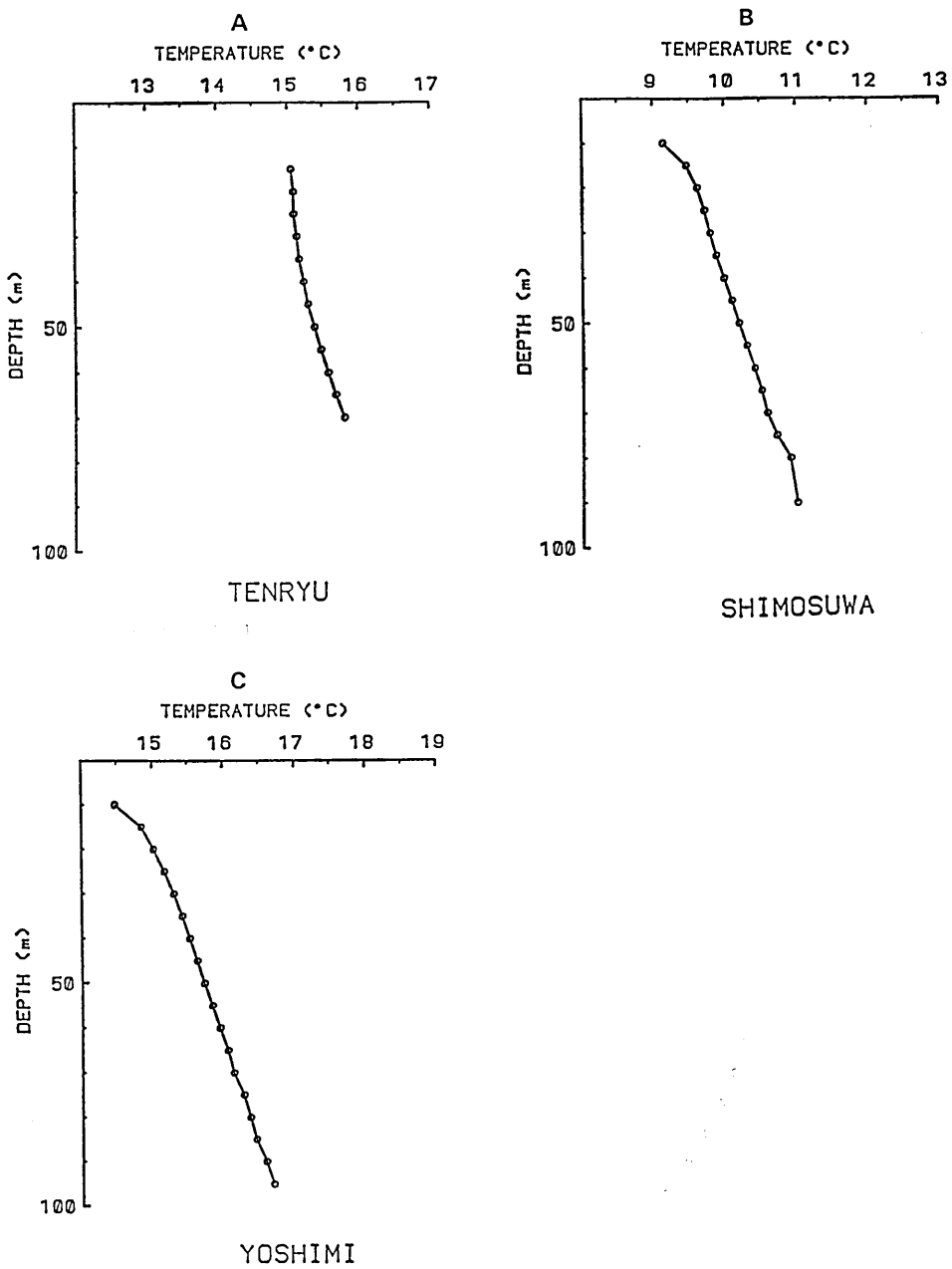

Fig. 5. Temperature-depth profiles for A) TENRYU; B) SHIMOSUWA; C) YOSHIMI.

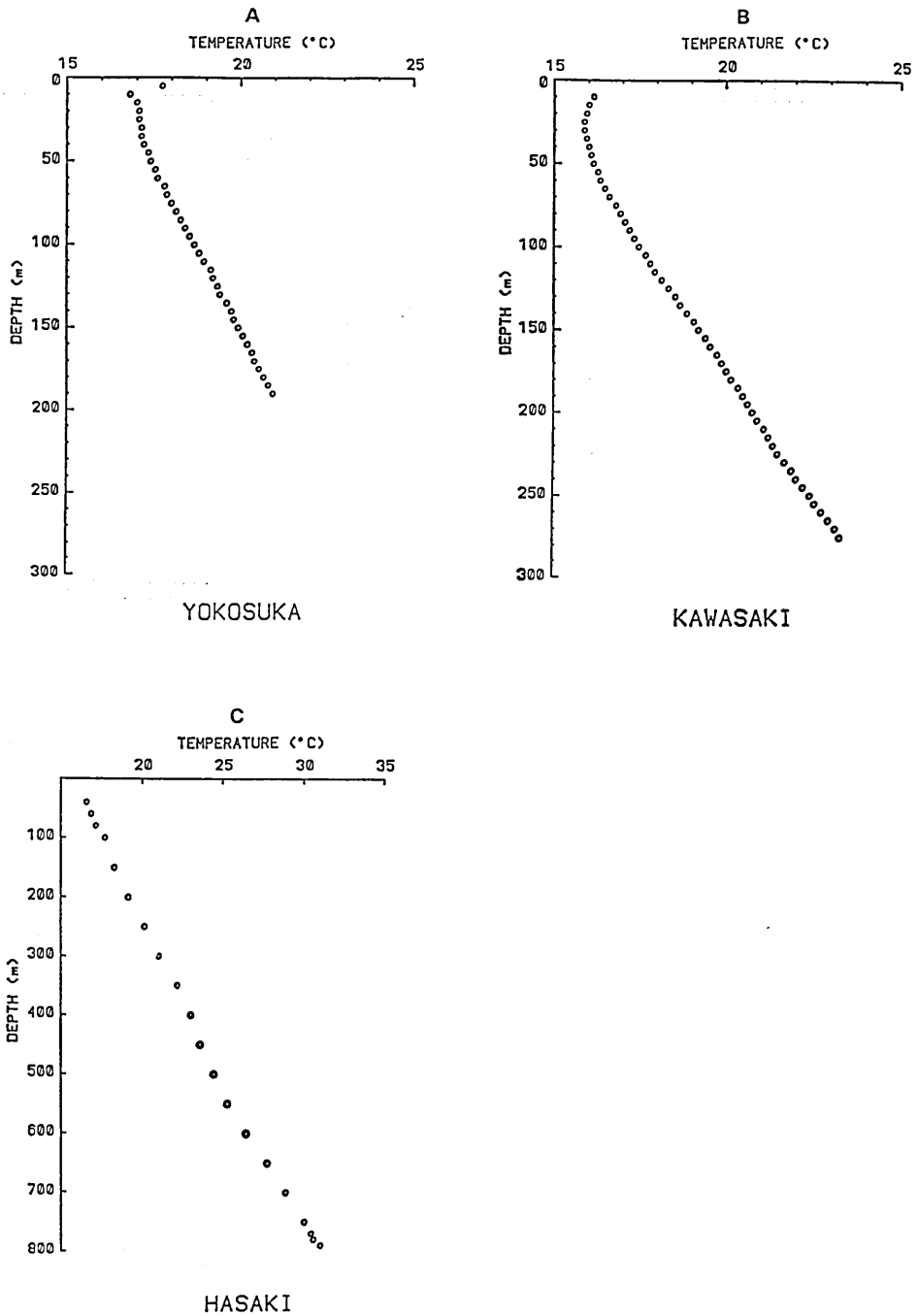

Fig. 6. Profiles of temperature-depth distribution for A) YOKOSUKA; B) KAWASAKI; C) HASAKI.

(7) Sudama

The site is situated at the junction between the east margin of the Fossa Magna and the west margin of the Kanto Mts.. The area is also in the east side of the Shimanto belt, consisting of Tertiary biotite granite, dykes of quartzporphyrite and andesite.

The hole, located at an altitude of 1350 m, is drilled through sediment cover at shallow depth but penetrates quartz-porphyrite rocks at a depth greater than 35 m. The depth of the hole is 108 m. Fig. 4-C illusrates the temperatures measured on June 18, 1987.

(8) Shimobe

The Itoigawa-Shizuoka Tectonic Line runs west of the site. West side of the Line the rocks are of Paleogene and creataceous age; on the east side they are of Neogene age. The locality is characterized by a thick sedimentary layer composed of alternative beds of mudstone and sandstone with about 1500 m in thickness.

Temperatures were measured to the 100 m depth on June 19, 1987. The lithology shown in the geological column is the same as the regional one. The temperature-depth profile is presented in Fig. 4-D.

(9) Tenryu

Geoiogically, the site belongs to the eastern part of the Shimanto belt. In the west side, the Komei fault and the Akaishi Tectonic Line are parallelly stretched out in N-S direction. The Itoigawa-Shizuoka Tectonic Line extends in the same N-S direction in the east side. The Mesozoic Mikura formation comprises most of the area.

Table 2. Heat flow data obtained from the drill-holes of NRCDP

Locality	Latitude (deg)	Longitude (deg)	Temp. grad. (mK/m)	Thermal cond. (W/mK)	Heat flow (mW/m^2)	Depth interval (m)
ACHI	35.4754	137.7380	12.1	3.14	38	35-90
HAMAOKA	34.6308	138.1592	31.2	1.21	38	20-90
HASAKI	35.8259	140.7355	17.3	1.20	21	50-780
HATSUSHIMA	35.0387	139.1715	17.2	1.64	28	35-70
KAWASAKI	35.5506	139.6792	31.9	1.36	43	35-190
KUSHIHARA	35.2576	137.4088	12.5	3.27	41	30-90
NUMAZU	35.1576	138.8462	20.7	2.80*	58	35-85
NIRAYAMA	35.0599	138.9628	70.8	1.97*	139	30-100
SUDAMA	35.8643	138.5770	61.3	2.02	124	15-100
SHIMOBE	35.4157	138.4834	101.5	2.17	220	40-92.5
SHIMOSUWA	36.1056	138.1328	20.5	3.08	63	20-90
TENRYU	34.9078	137.8852	20.2	3.93	79	45-70
YOKOSUKA	35.2077	139.6996	25.1	1.20	30	30-270
YOSHIMI	36.0477	139.4396	21.7	2.78	60	15-95

* Values from CERMAK and RYBACH (1982)

Table 3. Heat flow values provided by NEDO

Locality	Hole name	Latitude (deg. min.)	Longitude (deg. min.)	Temp. grad. (mK/m)	Thermal grad. (W/mK)	Heat flow (mW/^{2}m)	Depth interval (m)
KAISHIO	52E-KZ-1	36°13.0	137°32.7	155	3.15	488	158-1000
	52E-KZ-2			195	2.71	527	500-1000
ISHIZU	53E-ISZ-1	36°36.0	138°32.5	177	2.07	366	200-1265
	53E-ISZ-2			174	2.27	395	200-1270
YAKEDAKE	50-YD-1	36°13.0	137°23.5	150	2.70	405	500-800
	50-YD-2			50	3.04	152	501-803
	52-YD-3			235	2.91	684	258-604

Rocks in the hole are dominated by slate, with fine-grained sandstone interbedded. The logging depth is 80 m. Temperatures were measured on July 4, 1987. Fig. 5-A is the result of temperatures plotted versus depth.

(10) Shimosuwa

The site is near the Suwa Lake at 987 m in altitude. Except for a 5 m Quaternary sediment cover, granodiorite with phenocryst of quartz is the only rock type seen in the hole. Temperature determination was made to 103 m depth on June 18, 1987. Fig. 5-B shows the result.

(11) Yoshimi

The site is located at the east end of the Chichibu belt. The hole penetrates through amphibolite. Tempertures were determined to 100 m depth on Aprile 8, 1987. The profile of temperature-depth is shown in Fig. 5-C.

(12) Yokosuka

The 430 m deep drill-hole of Yokosuka is located in the Yokosuka city. The borehole penetrates Neogene mudstone only. We logged the temperatures on October 14, 1987. Fig. 6-A shows the temperature-depth profile in the hole.

(13) Kawasaki

The borehole is located in Kawasaki city. The area is composed mainly of Neogene sand-siltstones, covered with Quaternary sediments. The rock within the hole is mainly of sand-siltstone nature. Fig. 6-B shows the temperatures which was measured on October 14, 1987. In this site, since thermal conductivity has been measured by NRCDP, their results were used for determination of the heat flow.

(14) Hasaki

This site consists of Quaternary and Neogene sediments, mudstone and sandstone. These temperature data which are plotted in Fig. 6-C were provided by NRCDP.

The results from the above boreholes, including the temperature gradient, averaged thermal conductivity and heat flow, are listed in Table 2.

In addition, three data were provided by NEDO (the New Energy Development Organization). These data, which contain locality, hole name, thermal conductivity, temperature gradient, heat flow, are listed in Table 3.

3.4 Description of sites in areas of high topographic variation

The necessity of applying terrain correction to measured subsurface temperatures in areas of high topographic variations, such as those found near dam sites, has long been recognized in geothermal investigations (BIRCH, 1950; BLACKWELL *et al.*, 1980; HENRY and POLLACK, 1985). In this study, we approximated the topography of dam sites by two-dimensional geometry, using the method developed by NAGAO (1986) which is similar to that of HENRY and POLLACK (1985). Heat flow values were determined by mutiplying the corrected gradients by the harmonic mean thermal conductivity.

(1) Tokusa

Tokusa dam is iocated in the Nagano Prefecture. It is near the Median Tectonic Line and the Butsuzo Tectonic Line. No heat flow determination had been made near this site.

In November, 1987, temperature measurements were made in 7 drill-holes, rarely penetrating deeper than 100 m. Fig. 7 shows the location of all seven drill-holes logged and the temperature-depth profiles.

As seen in Fig. 7, the topography of this site can be approximated by two-dimensional geometry. The profile along the A1-A2 line is used for the correction model. Model configuration is shown in Fig. 8. Boundary conditions are: (1) specified surface temperature based on a linear relation between elevation and surface temperature, where available, detailed surface temperature obtained by extrapolation of temperature profiles observed at deeper part of drill-holes; (2) constant basal heat flux; (3) adiabatic boundaries on both sides. The grid contains 71 horizontal nodes and 50 vertical nodes; both horizontal and vertical spacing between nodes are 10 m.

On the basis of the model shown in Fig. 8, we did a series of numerical calculations varying only the basal heat flow, and compared the resulting nodal temperatures with measured values until a minimum squared deviation was established. The temperatures at the topographic surface nodes were set initially and held constant throughout the execution of the program. The temperature field for a given basal heat flow is determined by a iterative process, the process being ter-

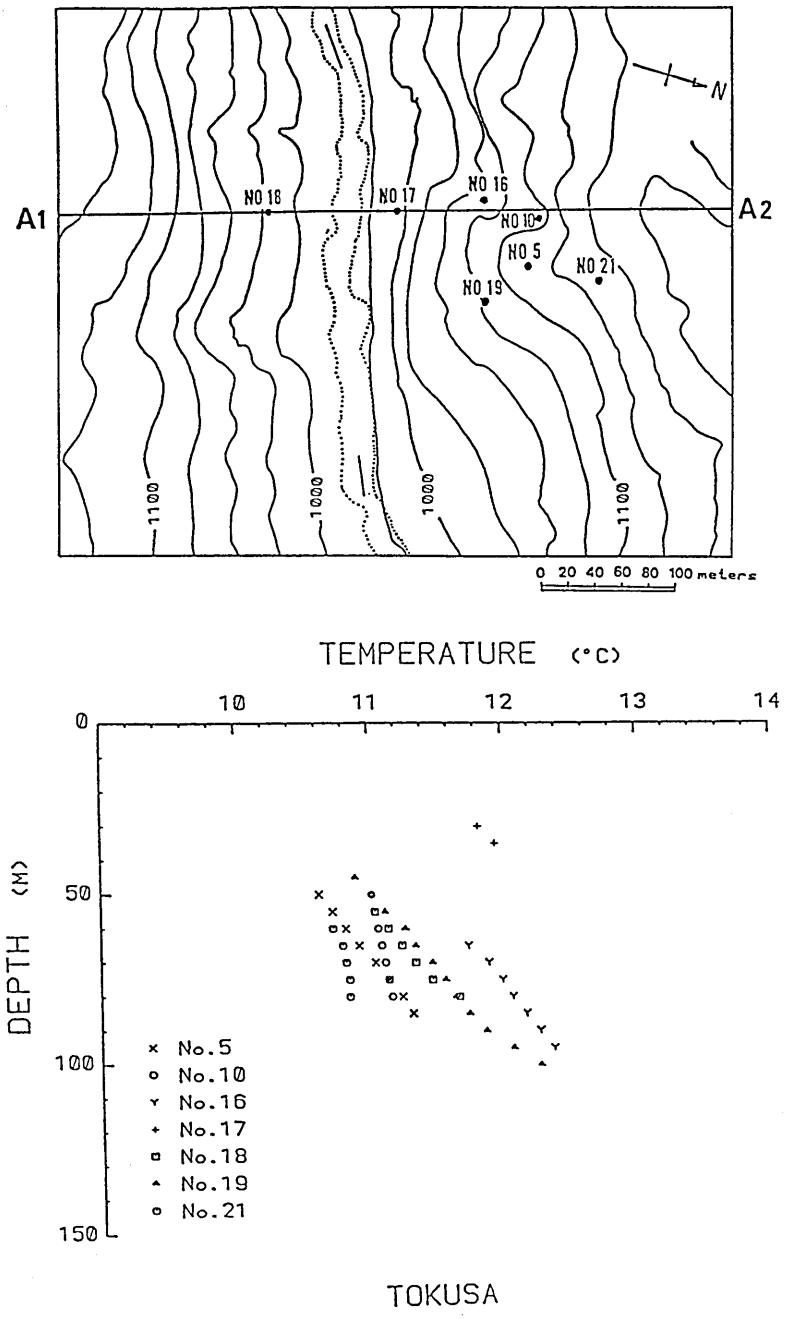

Fig. 7. Map showing the locations of all drill-holes in which temperature measurements were made at the Tokusa dam site. The dotted lines illustrate the valley filled with water and the arrows are the direction of water flow. Also shown are the location of the cross-section A1–A2 used for terrain correction. In the lower part are shown the results of temperature measurements for 10 drill-holes at the Tokusa dam site.

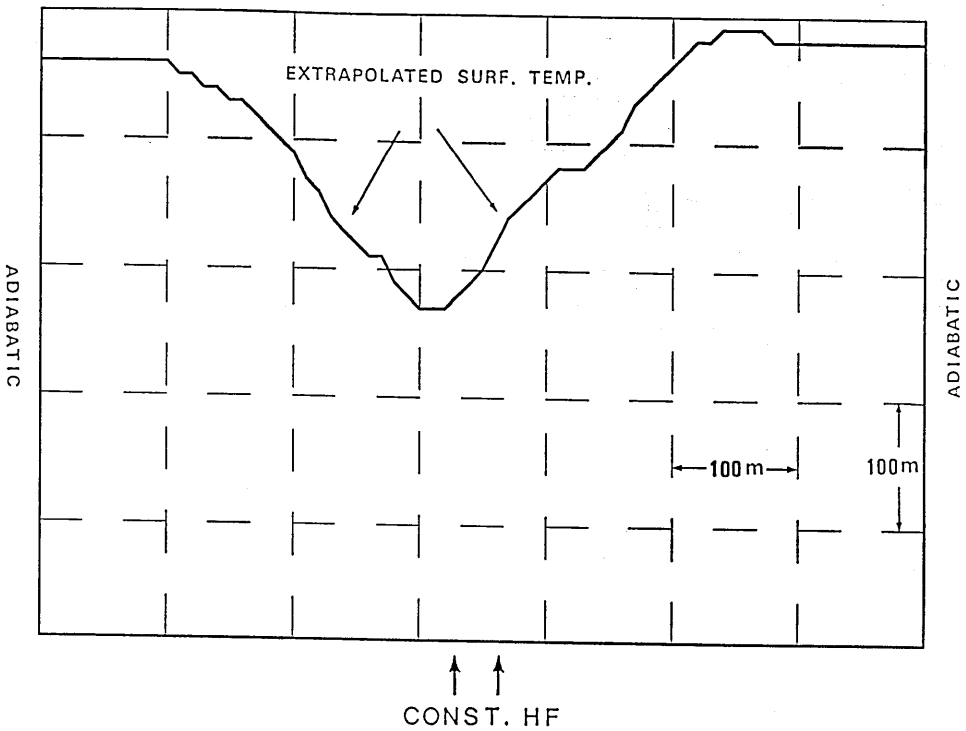

Fig. 8. Configuration of the model used for topographic correction to the case of the Tokusa dam site. Boundary conditions are as follows: 1) Both sides are adiabatic; 2) constant heat flux from below the bottom; 3) Surface temperature is given based on the extrapolation of the measured temperature gradient in the deeper part of holes.

minated when the maximum difference between temperatures determined from successive iterations for all nodes and the observed temperatures is less than 0.00002°C.

Some of the resulting temperature structures are shown in Fig. 9. The basal heat flows in these cases are 52, 65, 81, 91 and 104 mW/m^2 respectively. Fig. 10 is a plot of basal heat flux against residual which represents the mean-squared deviation between the observed and calculted temperatures at respective nodes. It is clear that the basal heat flow value of 81 mW/m^2 produces the best fit to the observed temperature field at this site.

(2) Maruyama

Temperature measurements were made in November, 1987. The locations of all the drill-holes logged and the cross-section along A1-A2 are shown in Fig. 11. Temperature-depth profiles at all boreholes are also presented in Fig. 11. Since the observed temperatures of hole

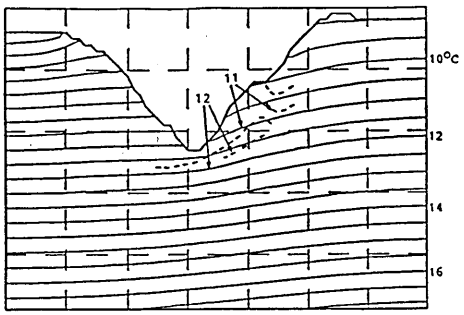

BASAL HEAT FLOW = 52
RESIDUAL = 0.17

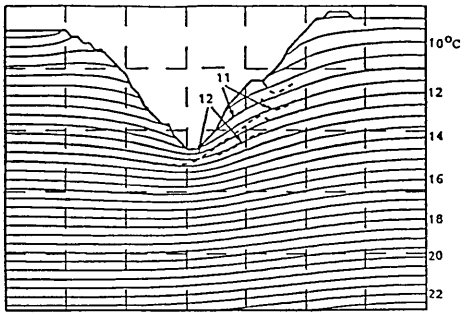

BASAL HEAT FLOW = 91
RESIDUAL = 0.13

BASAL HEAT FLOW = 65
RESIDUAL = 0.14

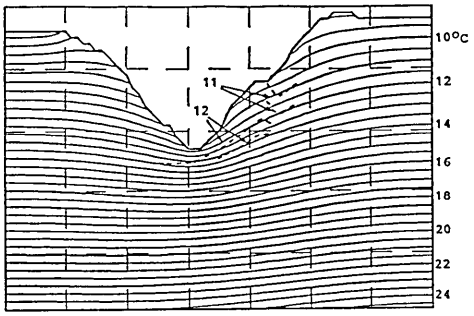

BASAL HEAT FLOW = 104
RESIDUAL = 0.15

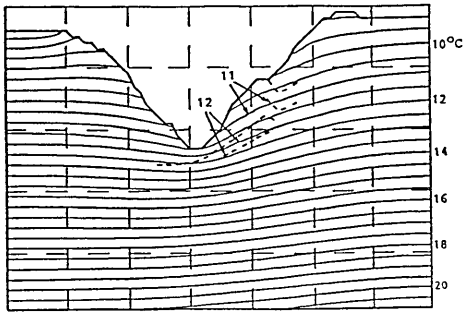

BASAL HEAT FLOW = 81
RESIDUAL = 0.12

$$\text{RESIDUAL} = \sqrt{\Sigma (T_{obs} - T_{cal})^2 / N}$$

Fig. 9. Five examples of numerical calculation for the above model. Basal heat flux is shown in the unit of mW/m^2. The definition of residual is illustrated at the bottom.

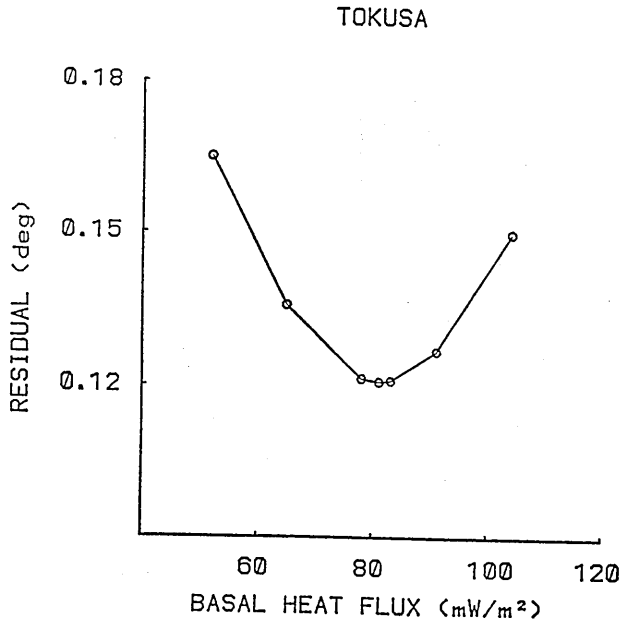

Fig. 10. The result of the calculated basal heat flux plotted versus residual. It is clear that the value of 81 mW/m² is the best in this case.

F-17 seem to be disturbed, we excluded the data of this hole from the topographic correction in this site. The same method as above was applied to make the topographic correction, resulting in the best heat flow value of 71 mW/m².

(3) Urayama

Temperatures were determined in 9 drill-holes ranging in depth from 60 to 100 m in September, 1987. Fig. 12 shows the location of the drill-holes logged and the cross-section used for the topographic correction. Also shown are the temperature-depth profiles for all drill-holes in this figure. A corrected heat flow value of 131 mW/m² was obtained.

(4) Yunishigawa

Temperatures were logged in 5 drill-holes ranging in depth from 70 to 155 m in July, 1987. Fig. 13 indicates the location of the drill-holes logged and the temperature-depth profiles. The temperature profile of drill-hole No. 4 has an abrupt leap at the depth of 90 m. There are two possible explanations for this. One could be associated with a sharp change of thermal conductivity at that depth. The other could be attributed to an existence of a fracture zone. The former can be ruled out because the geological column does not show

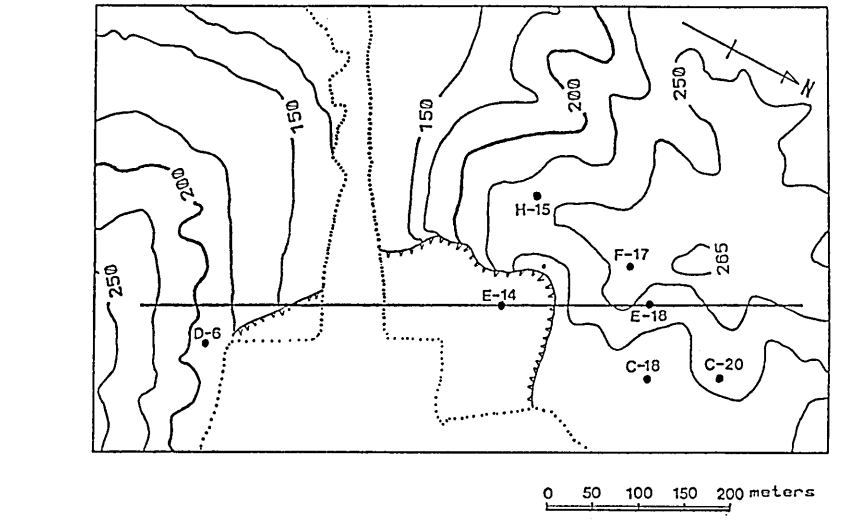

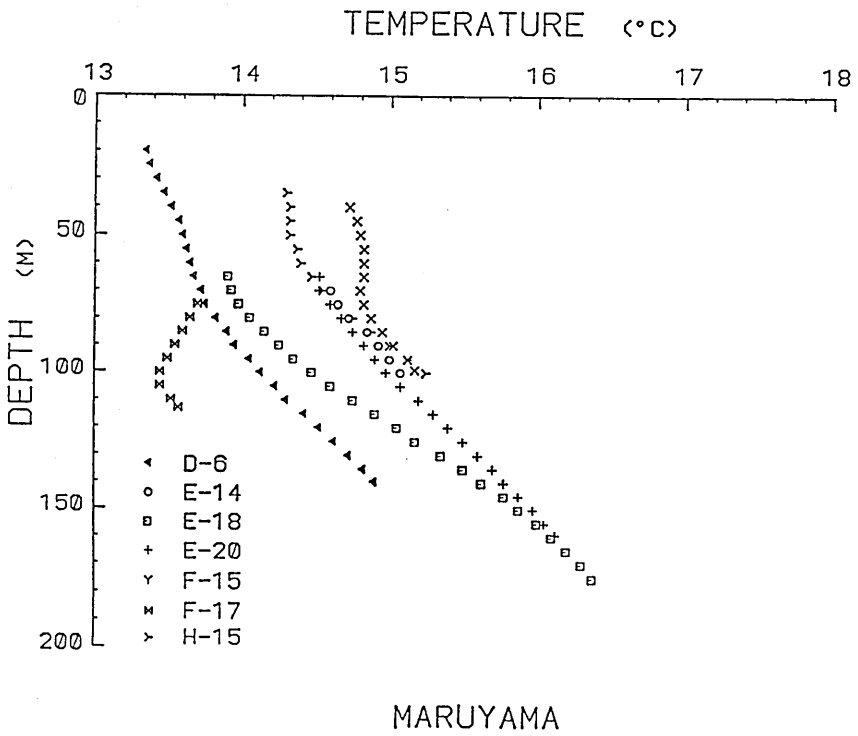

Fig. 11. Locations of all drill-holes logged in which temperature measurements were made at Maruyama (the upper part). Also shown is the location of the A1-A2 profile used for topographic correction. In the lower part, the measured temperature profiles are presented.

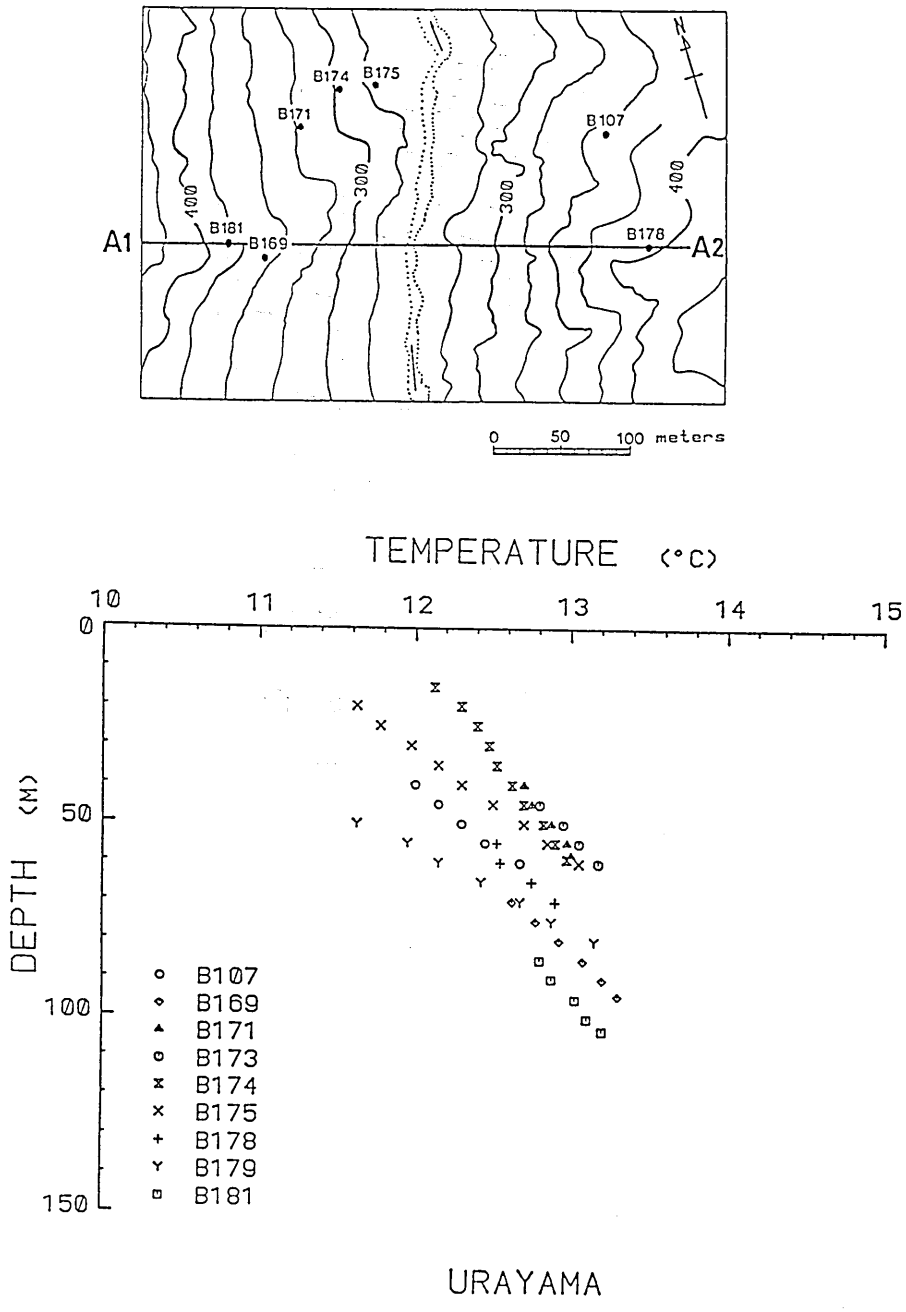

Fig. 12. Map showing the locations of all drill-holes logged at Urayama in the upper part. A1–A2 is the location of the profile used for topographic correction. In the lower part are illustrated the results of the temperature measurements.

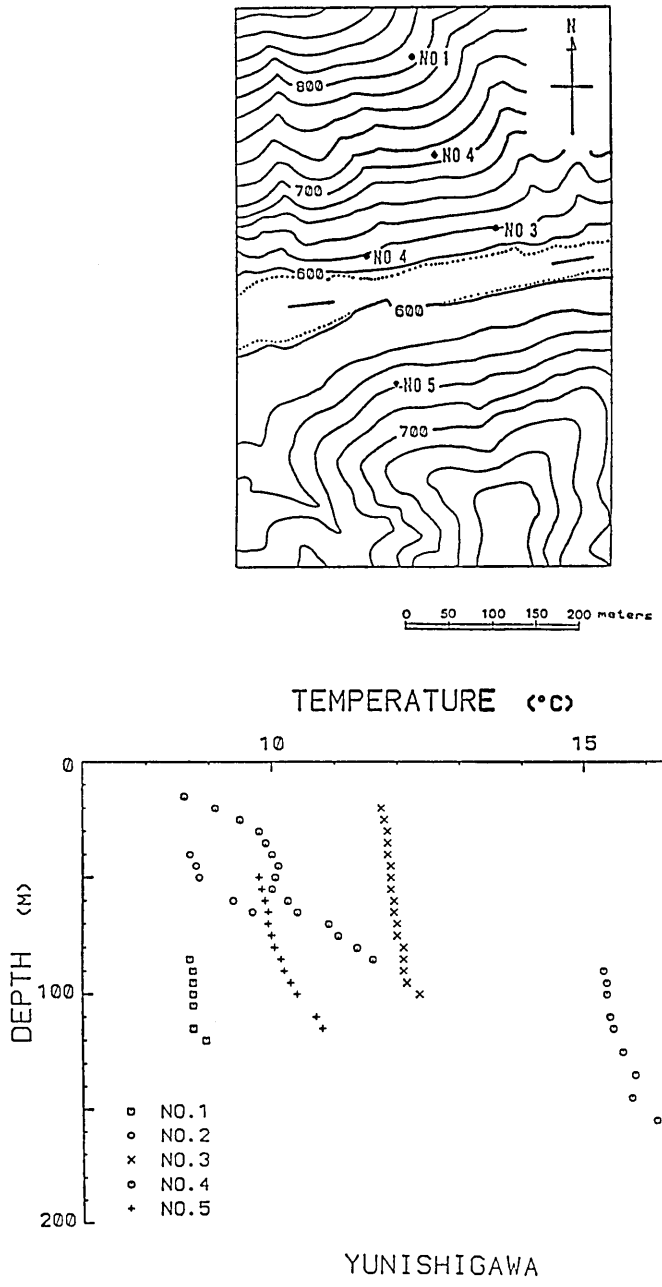

Fig. 13. Locations of the drill-holes logged at Yunishigawa (the upper part) and the temperature-depth profiles (the lower part).

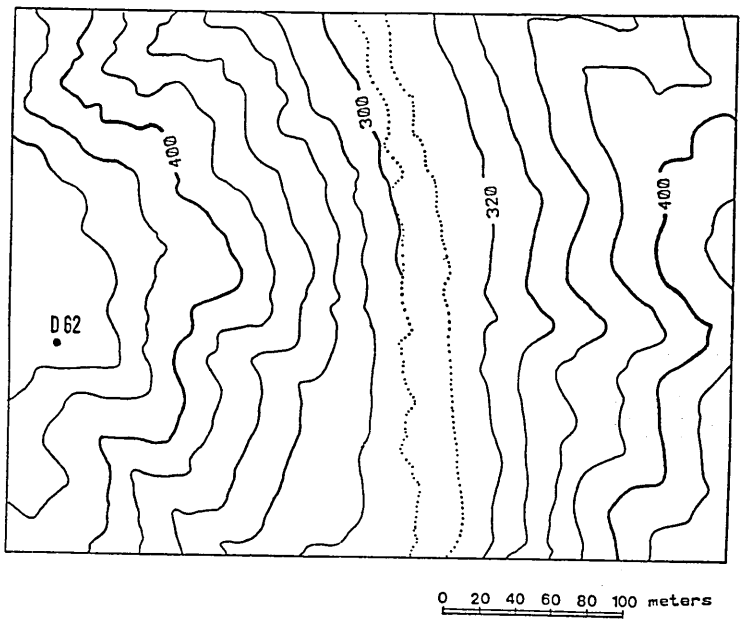

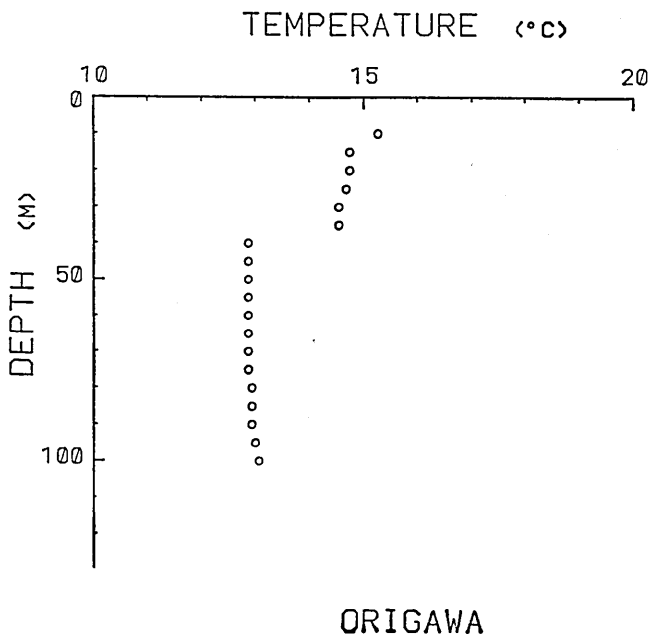

Fig. 14. Location of the drill-hole in which temperatures were made at Origawa (the upper part) and the temperature-depth profile obtained in D-62.

such a great change in lithology. This kind of temperature leap is also described by DRURY *et al.* (1984). They attributed it to a flow of water within a fracture zone. Since detailed lithologic logging data are not available, we used the other 4 temperature data and determined the heat flow as 33 mW/m^2.

(5) Origawa

We logged the temperatures only in one drill-hole as shown in Fig. 14. The result of temperature measurement is presented in the lower part of Fig. 14. The temperature gradient is determined as 8°C/km. The rock in the hole is composed of granite, which has a thermal conductivity of 3.2 W/mK. Since the data available are not sufficient to estimate the topographic effect, we did not determine the heat flow value in this site.

4. Disscusion

4.1 Contour map of surface heat flow distribution

From the above measurements and topographic corrections for the sites with high topographic variation, we obtained 18 new heat flow data in central Japan. In addition, 3 data are provided by NEDO in the region. Fig. 15 shows the new heat flow distribution map of central Japan.

Based on this map, we used an automatic contouring program to construct a contour map. Basically, the preparation method is the same as that described by CERMAK (1979). An upper limit of heat flow value, 120 mW/m^2, was imposed in the preparation of this contour map because of the fact that the heat flow values in this region are generally lower than 120 mW/m^2, except for areas of local thermal activity like geothermal fields and hot springs. So, it appears that the heat flow greater than 120 mW/m^2 is mainly related to local geothermal fields.

147 observed data were used in the area from 135 to 143° in longitude and 33 to 39°N in latitude, which is wider than the studied area, in order to minimize boundary effects. Data with low reliability were not included in preparing the map. Surely this number of data is small for a region with complicated thermal features like central Japan and the data coverage is certainly not uniform, but it is believed that, as the first approximation, it reflects regional anomalies reasonably well.

The resulting contour map is shown in Fig. 16. Contours are drawn at intervals of 20 mW/m^2. The thick solid lines illustrate the contours of 40 and 100 mW/m^2 respectively.

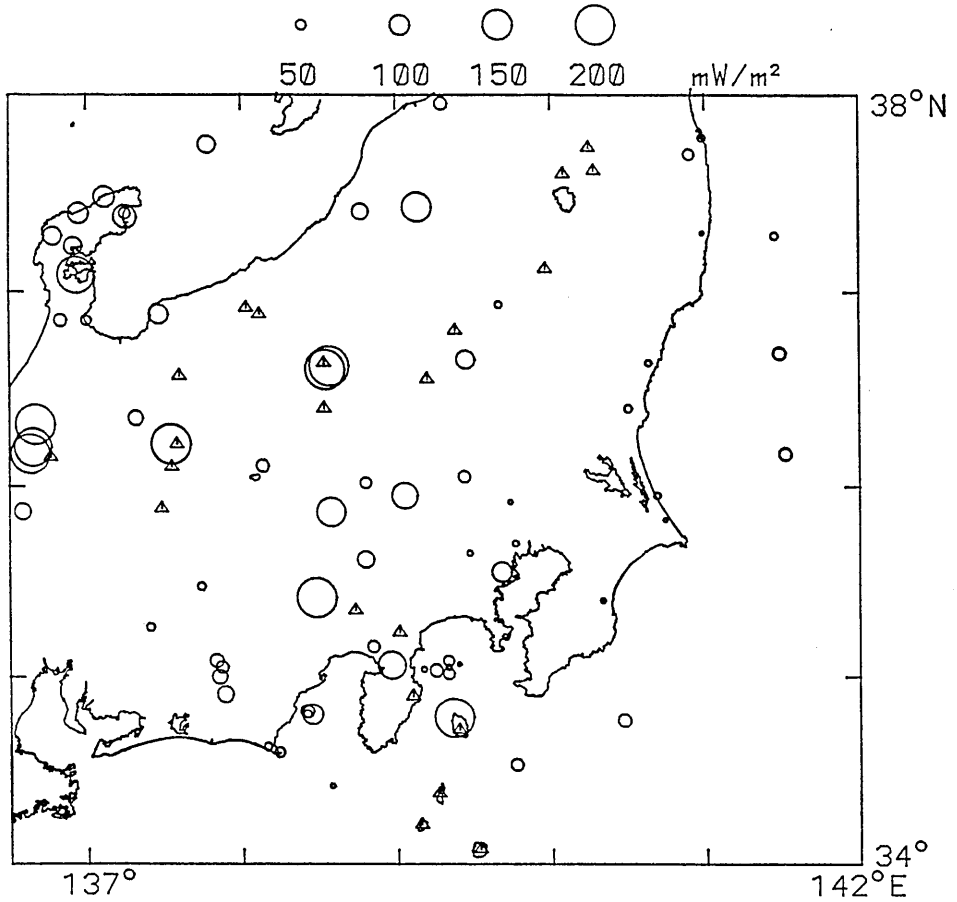

Fig. 15. New heat flow distribution map of central Japan. The diameter of the circles is proportional to their heat flow values. The triangles denote the Quaternary vocalnoes.

From the heat flow contour map, we can find two heat flow lows on land. A very broad zone of low heat flow is located in the central and eastern part of the Kanto district. This low heat flow zone may partly be attibuted to the sedimentation on the Kanto plain since this area has been a zone of intense subsidence since the Pliocene. LANGSETH *et al.* (1980) have made a graph for the sedimentation correction. We use their graph and the estimation of sedimentation rate 0.02 cm/Yr given by KAIZUKA (1987). Assuming constant heat flow from depth and constant sedimentation rate over the past 5 m.y., the observed heat flow will be reduced by only less than 10%. Therefore, the low heat flow itself is probably related to the tectonics in the

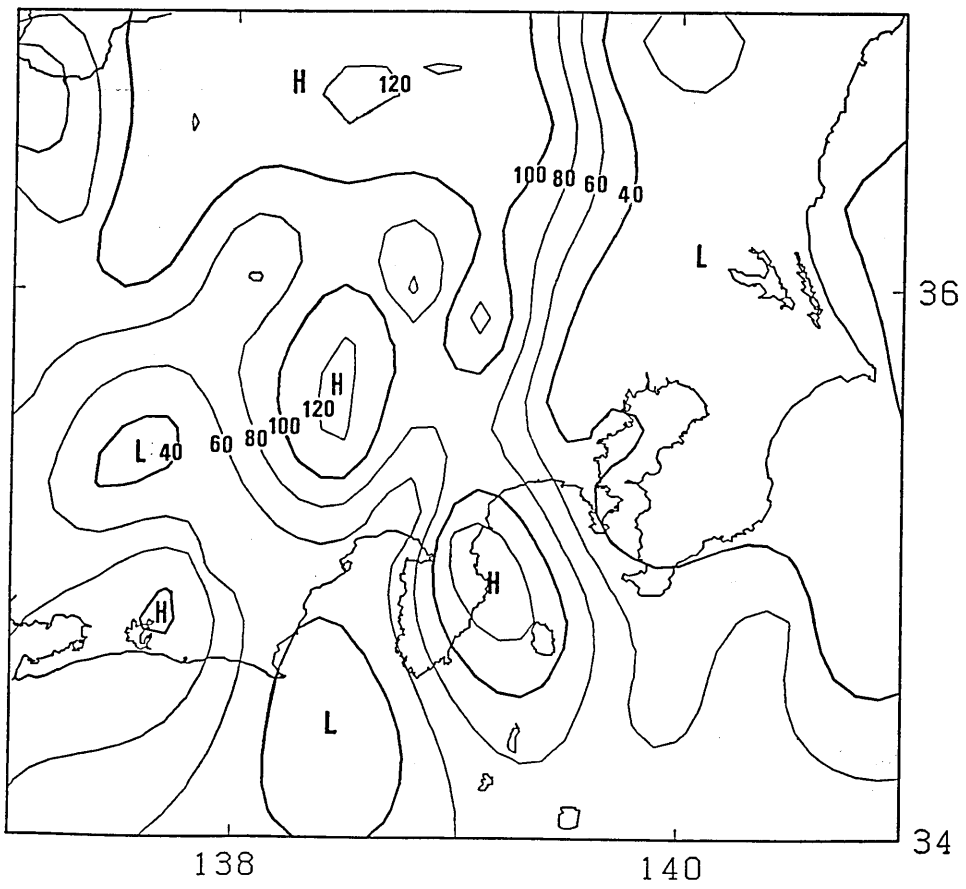

Fig. 16. A generalized heat flow distribution map of central Japan. Contours are drawn at 20 mW/m² intervals. H and L denote high and low heat flow areas respectively. The heat flow data (circles) used for the preparation of the contour map are illustrated in the figure.

region. Indeed, this area is situated between a trench to the east and a volcanic front to the west. The cooling of the subducting Pacific plate is likely to give rise to the low heat flow, just as seen in other subduction systems.

Another remarkable low heat flow is found in the western part of the Tokai district. It is easy to be understood if we consider the subduction of the Philipine Sea plate. But the heat flow distribution pattern is not so evident compared with other subduction systems. Partly, this may be disturbed by the nearby subduction system of the Pacific plate. More detailed heat flow measurement is necessary to

clarify the features in this region.

High heat flow anomalies are mainly distributed along the volcanic front and in areas of Quaternary volcanic activity. Those are most likely associated with the tectonic processes in the region, e.g., subduction of the Pacific plate and Philippine Sea plate.

4.2 Estimation of Moho-temperature and mantle heat flow

Heat flow through the surface of the earth includes several contributors: principally (1) subcrustal components which come from deeper structures (CHAPMAN and POLLACK, 1975; SCLATER *et al.*, 1980); (2) the heat coming from decaying radioactive elements within the crust, such as uranium, thorium and potassium (BIRCH *et al.*, 1968; LACHENBRUCH, 1970).

In order to quantify the sub-crustal components, it is necessary to subtract the crustal heat generation component. If we know the measured surface heat flow, radioactive heat generation and thermal conductivity of rocks, together with some assumptions on the crustal structure, temperature field can be estimated by using the thermal conduction equation.

$$c\rho\frac{\partial T}{\partial t}=\mathrm{div}\,(K\,\mathrm{grad}\,T)+A \qquad (1)$$

where K is thermal conductivity, A heat generation, c specific heat, ρ density, and T temperature.

Assuming steady-state condition and one-dimensional scheme, the above conduction equation can be simplified as,

$$\frac{d}{dz}\left(K\frac{dT}{dz}\right)+A=0 \qquad (2)$$

where Z is depth from the surface.

Three models have been proposed for the radioactive heat generation within the crust, i.e. constant distribution, linear

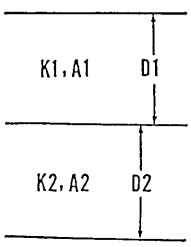

LAYER	K (W/mK)	A (μW/m)^3
1	3.0	1.4
2	2.0	0.6

Fig. 17. Two-layer model used for the estimation of the mantle heat flow and Moho-temperature. D_1, D_2 are the depth of each layer. The parameter values of K_1, K_2, A_1, A_2 are listed in the lower part of the figure.

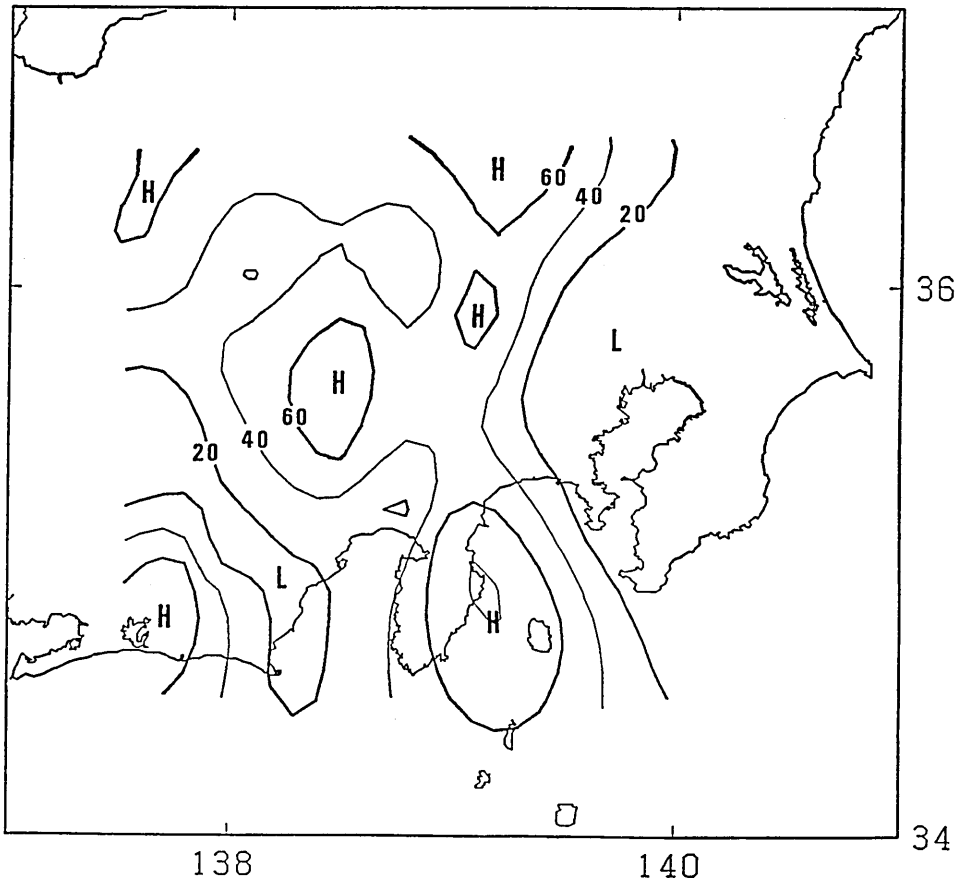

Fig. 18. Distribution of the estimated temperature at the Moho discontinuity. H and L denote the high and low temperatures respectively. The circles illustrate the surface heat flow values used in this calculation.

decrease and exponential decrease with depth. The exponential model $A=A_0\exp(-Z/D)$ seems to be the most likely one (LEE *et al.*, 1987). However, the parameters A_0 and D are difficult to be defined in a tectonically active terrain like Japan. For this reason, a two-layer model is used for simplicity (Fig. 17). In this model, each layer has constant radioactive heat generation with uniform thermal conductivity. These two layers are assumed to be the upper and lower crust with granitic (felsic) and basaltic (mafic) composition respectively. Thus, the mantle heat flow Q can be expressed as

$$Q=-A_2D_2+(Q_0-A_1D_1) \qquad (3)$$

Here, D_1, D_2, A_1, A_2 represent the depth and heat generation of the

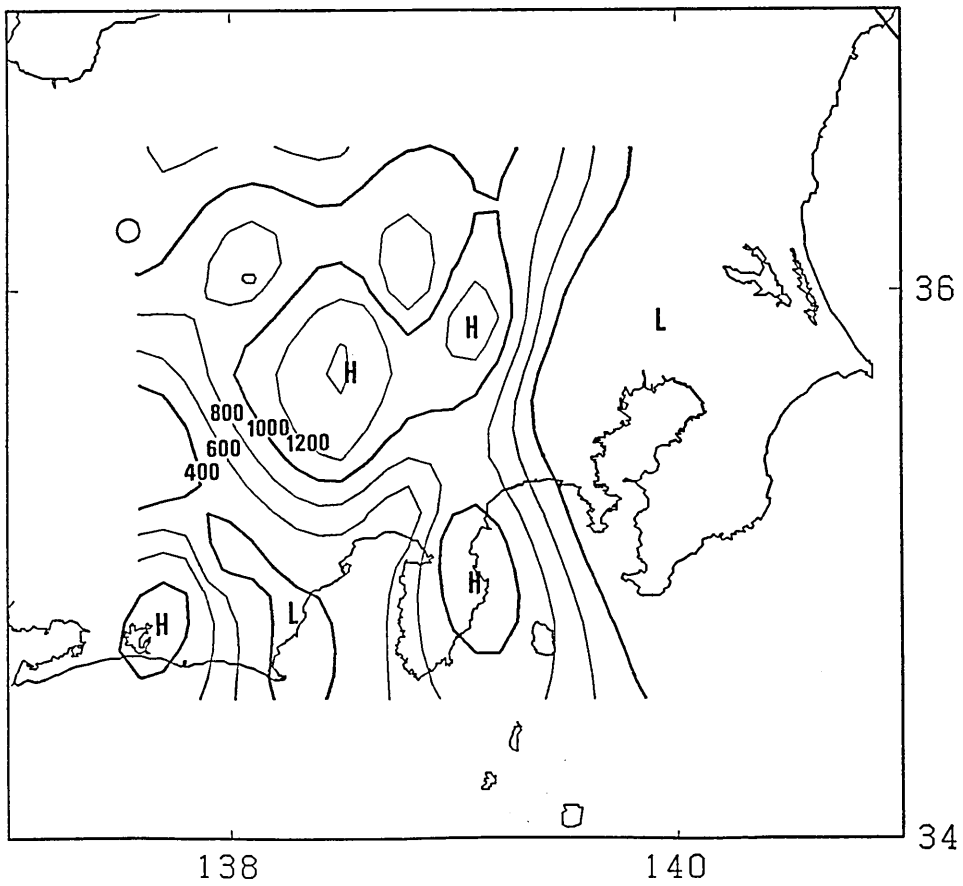

Fig. 19. Estimated mantle heat flow distribution at the Moho discontinuity. H and L indicate high and low values respectively. The circles illustrate the same mean as above.

first layer and second layer respectively, and Q_0 is the surface heat flow. The values of the parameters A_1, A_2 are presented in this figure. The data of D_1, D_2 are adopted from ASHIYA *et al.* (1987).

On the basis of the above formula, the mantle heat flow Q at each observation point was calculated and its contour map was prepared using the same technique as that for the surface heat flow (Fig. 18).

The map indicates that the mantle heat flow varies in a great range, but its distribution pattern is similar to that of the surface heat flow. This suggests that the regional high heat flow is due not to the thick crust, but to the deep origin. This deep origin is likely to be related to the tectonic evolution and mantle convection.

Moho-temperature can be obtained by solving equation (2):

$$T = -A_2D_2^2/2K_2 + (Q_0 - A_1D_1)D_2/K_2 + (-A_1D_1^2/2K_1 + Q_0D_1/K_1) \quad (4)$$

Here, K_1 and K_2 represent the conductivity of the first layer and second layer respectively. Based on the formula, the Moho-temperature at each obsvervation point was calculated. Then, we constructed the coutour map shown in Fig. 19. Contour interval is 200°C. The Moho-temperature also varys greatly in a range from 200 to 1200°C. These variabilities of the mantle heat flow and Moho-temperature support the conclusion given by CERMAK (1982) that the Moho discontinuity is neither an isothermal surface nor a constant heat flow surface. Both of these quantities vary in broad ranges.

4.3 A comparison of heat flow and Curie-point depth distribution

The Curie temperature is that at which a magnetic mineral loses

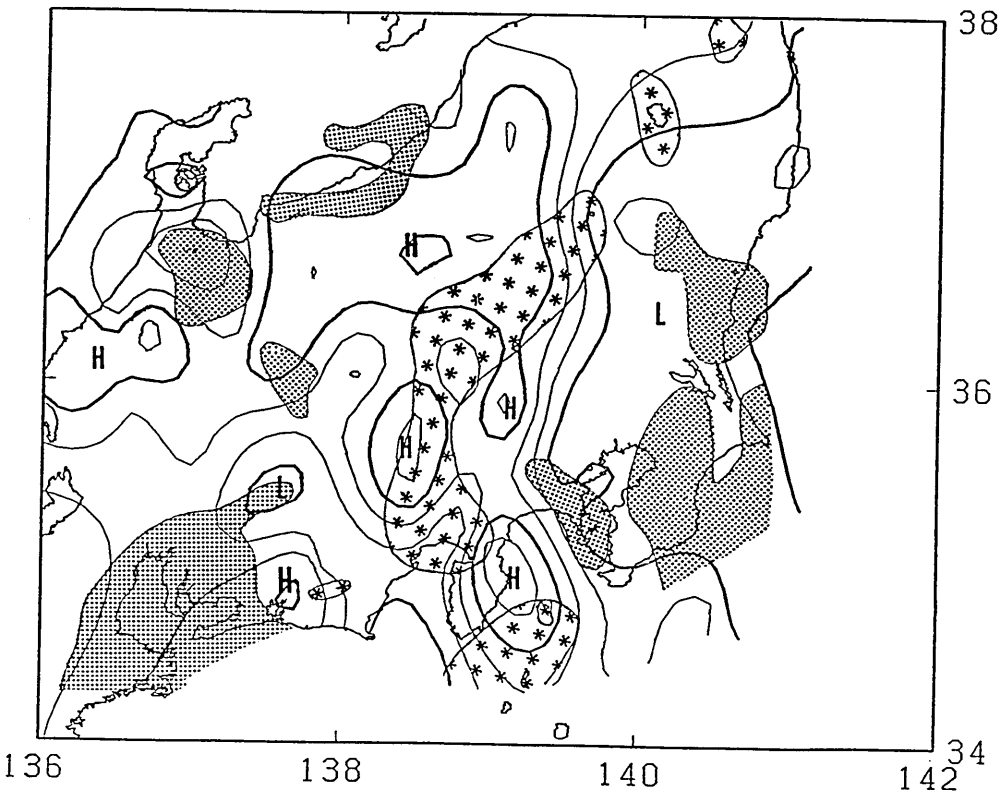

Fig. 20. Regional heat flow and Curie point depth. The starmarked and shaded portions denote areas of shallow (<8 km) and deep (<20 km) Curie point depths respectively.

its ferromagnetism. In rocks of the earth's crust, Fe-Ti oxide mineral series are abundant and attain large magnetization values and are the predominant sources of observed anomalies (MAYHEW, 1982). The Curie temperature of any such magnetic mineral is reached at variable depths due to lateral variations in temperature gradients. Thus it should be of interest to investigate the relation between measured heat flow and the Curie isotherm since it could be helpful in the assessment of geothermal resources and the understanding of geothermal structures as the first approximation, particularly where heat flow data are not available.

OKUBO (1984) has presented the Curie isotherms for this region. We used his results to compare our heat flow distribution obtained in this study. Fig. 20 shows the superimposed distributions of the two data sets. The shaded portions denote areas where the Curie point depth is deeper than 20 km, while the star-marked portions illustrate areas shallower than 8 km. The heat flow distribution contour map is the same as in Fig. 16. On the whole, good correlation can be seen in the area, i.e., the areas of high heat flow correspond to those of shallow Curie point depth.

4.4 Comparison of heat flow distribution with seismic velocity perturbations and attenuation structures

It is well known that the v_p seismic-wave velocities in the individual crustal layers depend not only on petrological composition but also on *in-situ* pressure-temperature conditions. With increase of temperature velocity decreases, pressure has an effect in the opposite sense, but usually temperature is the dominating factor in this respect. Therefore, it should be interesting to compare velocity structure with thermal structure.

ISHIDA and HASEMI (1988) have investigated the P-wave velocity structure in different depth ranges beneath the Kanto-Tokai district by applying an inversion method for local earthquake data. This allows us to make an comparison of their fractional velocity perturbations of deep temperatures obtained in this study.

Compared with their velocity structures at different depths, it was found that the seismic velocity perturbations at the depths of 16-47 km are the most consistent with the heat flow distribution. The result is shown in Fig. 21. The shaded portions illustrate the areas of high velocity anomaly, while the starmarked portions show the areas of lower velocity. The relation between the velocity structure and the surface heat flow is not so remarkable although the low velocity zones coincide quite well with the high heat flow areas. At other depths,

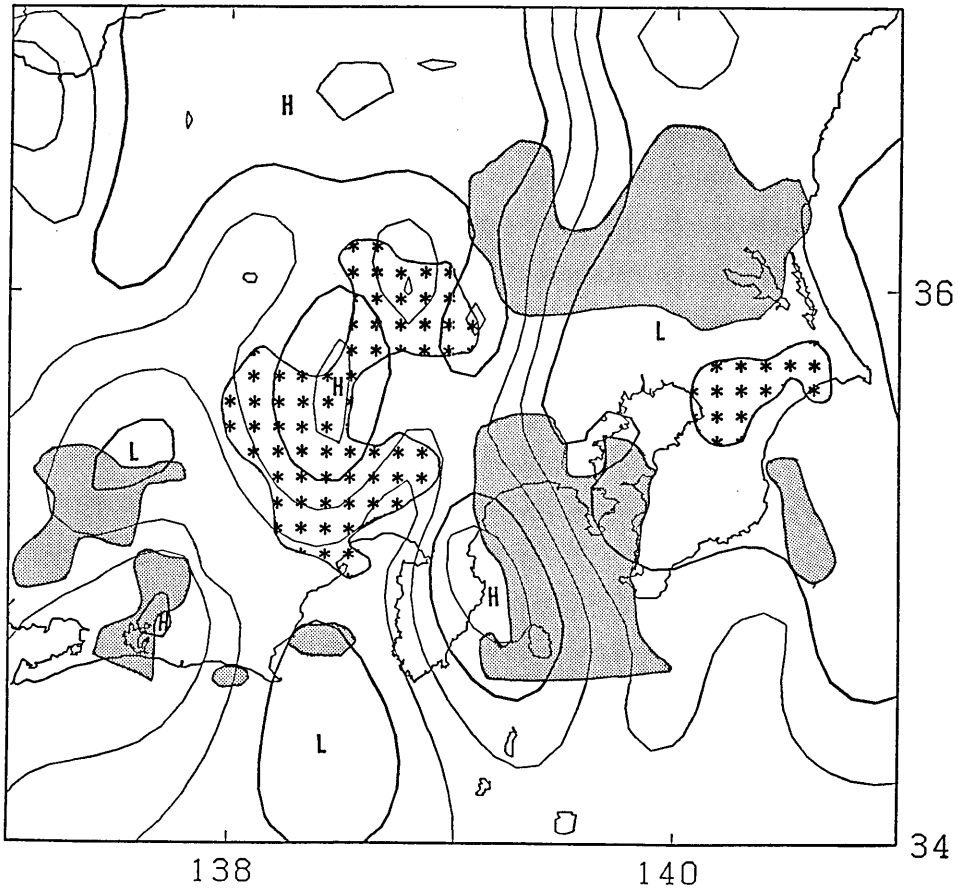

Fig. 21. Regional heat flow distribution and velocity structure in the depth range of 16–47 km (from Ishida and Hasemi, 1988). The star-marked and shaded portions indicate the low and high velocity areas respectively. The heat flow contour map is the same as Fig. 16.

the relation is weaker.

Seismic-wave attenuation is another quantity that may be related to temperature. Using seismic intensity data, HASHIDA (1987) has investigated the three-dimensional attenuation structure beneath the Kanto-Tokai district. His results show that the seismic quantity factor, Q, in the upper mantle sharply decreases towards the volcanic front of Honshu. The subducting Phillippine Sea plate, on the other hand, is marked out by a high-Q layer. In this study, we compared our thermal distribution with the attenuation structures in different depth ranges. On the whole, the variation of seismic attenuation in this area seems to correspond well to those of the ther-

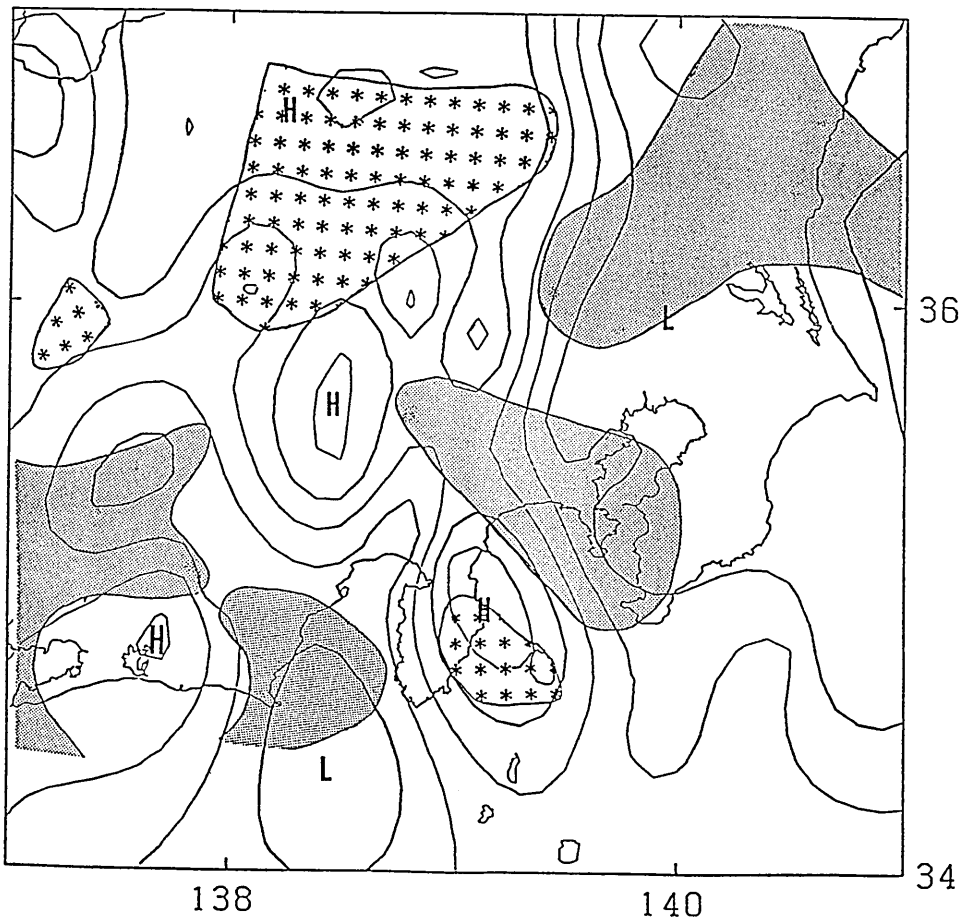

Fig. 22. Regional heat flow distribution superimposed by attenuation structure for the layer of 30-60 km depth (from Hashida, 1987). The star-marked portions show areas where attenuation is strong, while the shaded portions represent areas of weak attenuation.

mal field, particularly in the depth range of 30-60 km (Fig. 22).

4.5 Correlation between heat flow and seismicity

The distribution of earthquakes with depth depends on physico-mechanical characteristics of rocks which may be related to the thermal state of the crust and upper mantle. Thus, the focal depth is controlled by temperature to a great degree (CHEN and MOLNAR, 1983, KONDORSKAYA and KIREYEV, 1985, DOSER and KANAMORI, 1986).

In order to elaborate the possible relation between thermal state and distribution of focal depth, we used the earthquake data recorded

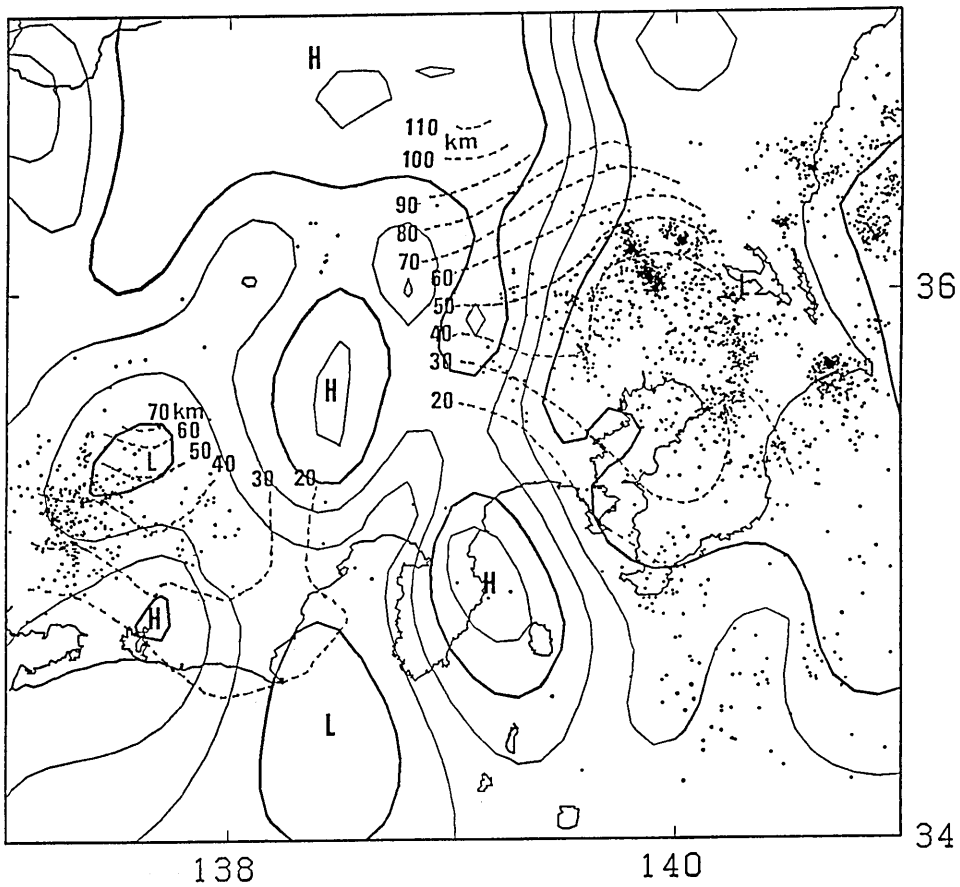

Fig. 23. The regional heat flow and distribution of seismic epicenters in the layer of 40-60 km depth for the period of 1983-1985. The seismicity data are provided by the National Research Center for Disaster Prevention. The dotted contour lines indicate the upper surface of the Philippine Sea plate (after Yamazaki and Ooida, 1985, Noguchi, 1985).

on the Kanto-Tokai seismic network by NRCDP in the period of 1983-1985. Different focal depths were selected and compared with thermal state. It is found that the focal depth between 40 and 60 km is in the best agreement. Fig. 23 represents the heat flow and earthquake distribution in the depth range of 40-60 km. In this figure, there obviously exists a zone of absence of earthquakes in the eastern part of the Tokai district. This low seismicity zone is consistent with the high heat flow. However, this correlation is not strong at other depth ranges.

We further use the depth contours of the upper surface of the Phillippine Sea plate compiled by NOGUCHI (1985) and YAMAZAKI and

OOIDA (1985). Interestingly, the area where the contours are absent coincides with the heat flow high. It is inferred that high temperature may induce aseismic creep, leading to an apparent absence of the Phillippine Sea plate in this region, rather than no existence of the slab.

5. Conclusions

Heat flow measurements were made in central Japan. The results show the following features of the heat flow distribution in this area.

1) Heat flow is low through the central to eastern part of the Kanto district.

2) Heat flow increases sharply towards the volcanic front up to over 100 mW/m^2.

3) There exists a heat flow low in the western part of the Tokai district.

Those features can be mainly interpreted as being associated with the subduction of the Pacific plate and Philippine Sea plate respectively.

Under the assumption of two-layer crustal structure, the Moho-temperature and mantle heat flow were estimated by using one-dimensional steady-state conduction equation. The results indicate that the distribution patterns of the Moho-temperature and mantle heat flow are similar to that of the surface heat flow. This substantiates the hypothesis that the Moho-discontinuity is neither an isothermal surface, nor is a constant heat flow surface.

The heat flow distribution was compared with that of the Curie point depth, velocity perturbations, seismic attenuation and seismicity. Similarity is found between the heat flow and Curie point depth. The correlation between the distribution of the heat flow and that of velocity perturbations is not so remarkable while the relation with seismic attenuation at the depth around the Moho is quite good.

Correlation of the heat flow and seismicity was also examined by using the data recorded by the Kanto-Tokai seismic network of NRCDP. It was found that there is no significant seismicity in the depth range of 40–60 km where heat flow is high, while it is assumed that at these depths in this region the upper surface of the subducting Philippine Sea plate is present.

Acknowledgement

We are very grateful to Dr. M. Ishida for providing the seismicity data in the studied region. Dr. O. Matsubayashi is acknowledged for

giving us three heat flow data and valuable ideas. Special thanks are given to the scientists and officials of the Water Resources Development Public Cooperation, the Kanto Regional Construction Bureau and the Chubu Regional Construction Bureau for their kind guidance to make the measurements possible.

References

ASHIYA, K., S. ASANO, T. YOSHII, M. ISHIDA, T. NISHIKI, 1987, Simultaneous determination of the three-dimensional crustal structure and hypocenters beneath the Kanto-Tokai district, *Tectonophysics*, **140**, 13-27.

BIRCH, F., R. F. ROY, and E. R. DECKER, 1968, Heat flow and thermal history in New York and New England, in "Studies of Appalachian Geology: Northern and Maritime", (E. Zen, W. S. White, J. B. Hadley, J. B. Thompson, eds.), pp. 437-451, Wiley-Interscience, New York.

BIRCH, F., 1950, Flow of heat in the Front Range, Colorado, *Bull. Geol. Soc. Am.*, **61**, 567-630.

BLACKWELL, D. D., J. L. STEELS, and C. A. BROTT, 1980, The terrain effect on terrestrial heat flow, *J. Geophys. Res.*, **85**, 4757-4772.

CERMAK, V., 1979, Heat flow map of Europe, in "Terrestrial Heat Flow" (V. Cermak, and L. Rybach, eds.), Springer-Verlag, Berlin Heidelberg, New York.

CERMAK, V., 1982, Crustal temperature and mantle heat flow in Europe, *Tectonophysics*, **83**, 123-142.

CERMAK, V., and L. RYBACH, 1982, Thermal properties, in "Physical Properties of Rocks" (G. Angenheister, eds.), Springer Verlag, Berlin, Heidelbers and New York, 305-481.

CHAPMAN, D. S., and H. N., POLLACK, 1975, Global heat flow: a new look, *Earth Planet. Sic. Lett.*, **28**, 23-32.

CHEN, W. P., P. MOLNAR, 1983, Focal depth of intracontinental earthquakes and their implications for the thermal and mechanical properties of the lithosphere, 1983, *J. Geophs. Res.*, **88**, 4183-4314.

DOSER, D. I., and H. KANAMORI, 1986, Depth of seismicity in the Imperial Valley region (1977-1983) and its relationship to heat flow, crustal structure, and the October 15, 1979 earthquake, *J. Geophys. Res.*, **91**, 675-688.

DRURY, M. J., and A. M. JESSOP, and T. J. LIWIS, 1984, The detection of groundwater flow by precise temperature measurements in boreholes, *Geothermics*, **13**, 163-174.

EHARA, S., 1984, Thermal structure and seismic activity in central Kyushu, Japan, *Jour. Volcanol.*, **29**, 75-94 (in Japanese with English abstract).

FURUKAWA, Y., and S. UYEDA, 1986, Thermal state under Tohoku Arc with consideration of crustal heat generation, *Jour. Volcanol.*, **31**, 15-28 (in Japanese with English abstract).

HASHIDA, T., 1987, Determination of three-dimensional attenuation structure and source acceleration by inversion of seismic intensity data: Japanese Islands, *Bull. Earthq. Res. Inst.*, **62**, 247-287.

HENRY, S. G., and H. N. POLLACK, 1985, Heat flow in the presence of topography: Numerical analysis of data ensembles, *Geophysics*, **50**, 1135-1341.

HONDA, S., Y. MATSUBARA, T. WATANABE, S. UYEDA, K. SHIMAZAKI, K. NOMURA, and N. FUJII, 1979, Compilation of eleven new heat flow measurements on the Japanese Islands, *Bull. Earthq. Res. Inst.*, **54**, 45-73.

HONDA, S., and UYEDA, 1984, Thermal structure beneath Tohoku, northeast Japan—a case study for understanding the detailed thermal structure of subduction zone, *Tectono-*

physics, **112**, 69-102.

HORAI, K., and S. UYEDA 1963, Studies of the thermal state of the earth, The 13th paper: Terrestrial heat flow in Japan, *Bull. Earthq. Res. Inst.*, **42**, 93-132.

ISHIDA, M., and A. HASEMI, 1988, Three-dimensional fine velocity structures and hypocentral distribution of earthquakes beneath the Kanto-Tokai district, Japan, *J. Geophys. Rec.*, **93**, 2076-2094.

KAIZUKA, S., 1987, Quaternary crustal movements in Kanto, Japan, *Journal of Geography.*, **96-4**, 51-68 (in Japanese with English abstract).

KONDORSKAYA, N. V., and I. A. KIREYEV, 1985, On the estimation of earthquake maximum magnitude based on a joint analysis of seismological and geothermal parameters, *Tectonophysics*, **121**, 79-85.

KONO, Y., and Y. KOBAYASHI, 1971, Terrestrial heat flow in Hokuriku district, Central Japan, *Sci. Rep. Kanazawa Univ.*, **16**, 61-72 (in Japanese).

LACHENBRUCH, A. H., 1970, Crustal temperature and heat production: implications of the linear heat-flow relation, *J. Geophys. Res.*, **17**, 3291-3300.

LACHENBRUCH, A. H., and J. H. SASS, 1978, Heat flow in the United States and the thermal regime of the crust, in "the Earth'Crust" (J. G. Heacock ed.), Geophys. Monogr. Ser, Vol. 20, American Geophysical Union, Washington, D. C.

LANGSETH, M. G., M. A. HOBART, and K. HORAI, 1980, Heat flow in the Bering Sea, *J. Geophys. Res.*, **85**, 3740-3750.

LEE, M. K., G. C. BROWN, P. C. WEBB, J. WHEILDON, and K. E. ROLLIN, 1987, Heat flow, heat production and thermo-tectonic setting in mainland UK, *J. Geolog. Sco.*, **144**, 35-42.

MATSUDA, T., 1978, Collision of the Izu-Bonin arc with central Honshu: Cenozoic tectonics of the Fossa Magna, Japan, *J. Phys. Earth*, **26**, S 409-S 421.

MAYHEW, M. A., 1982, Application of satellite magnetic anomaly data to Curie isotherm mapping, *J. Geophys. Res.*, **87**, 4846-4854.

NAGAO, T., 1986, Heat flow measurements in the Tohoku-Hokkaido regions by some new techniques and their geotectonic interpretation (Doctor Thesis).

NAKAMURA, K., H. SHIMAZAKI, N. YONEKURA, 1984, Subduction, bending and eduction. Present and Quaternary tectonics of the northern border of the Philippine Sea plate, *Bull. Soc. Geol. France*, **7**, 224-243.

NIITSUMA, N., and T. MATSUDA, 1985, Collision in the south Fossa Magna area, central Japan, in "Lithospheric studies in and around Japan" (Akimoto, S., S. Uyeda, and M. Kono, eds.), pp. 41-50, DELP Publication No. 3, Tokyo.

NOGUCHI, S., 1985, Configuration of Philippine Sea plate and characteristics of seismicity in Ibaragi area. *The Earth Monthly*, **7**, 97-104 (in Japanese).

OKUBO, Y., 1984, Curie point depths over the whole Japan, *Geological news*, **362**, 12-17.

POLLACK, H. N., and D. S. CHAPMAN, 1977, On the regional variation of heat flow, geotherms, and lithospheric thickness, *Tectonophysics*, **38**, 279-296.

SASS, J. H., A. H. LACHENBRUCH, and R. J. MUNROE, 1984, Thermal conductivity determinations on solid rock—a comparision between a steady-state divided-bar apparatus and a commercial transient line-source device, *J. Volcanol. Geotherm. Res.*, **20**, 145-153.

SCLATER, J. G., C. JAUPART, and D. GALSON, 1980, The heat flow through oceanic and continental crust and the heat loss of the earth, *Rev. Geophys. Space Phys.*, **18**, 269-311.

UYEDA, S., and K. HORAI, 1964, Studies of the thermal state of the Earth, the eighth paper: Terrestrial heat flow measurements in Kanto and Chubu districts, Japan, *Bull. Earthq. Res. Inst.*, **41**, 83-107.

UYEDA, S., 1972, Heat flow, in the Crust and Upper Mantle of the Japanese Area, Part 1, Geophysics, Earthquake Res. Inst., Chapter 5, 96-105.

WATANABE, T., M. LANGSETH, and R. N. ANDERSON, 1977, Heat flow in back-arc basins of the Western Pacific, in "Island Arcs, Deep Sea Trenches and Back-arc Basins", (M.

Talwani, and W. C. Pitman, eds.), pp. 137-167, Maurice Ewing Ser., Vol. 1, American Geophysical Union, Washington, D. C.

YAMAZAKI, F., T., OOIDA, 1985, Configuration of subducted Philippine Sea plate beneath the Central region, Central Japan, *Zisin*, 38, 193-201 (in Japanese witk English abstract).

中部日本の地殻熱流量及び他の観測データとの相関性

地震研究所 李 新元 / 古川善紹 / 長尾年恭* / 上田誠也

国立防災センター 鈴木宏芳

国立防災科学技術センターの関東-東海地震観測ネットワークのボーリング孔と水資源開発公団，関東地方建設局，中部地方建設局地質調査用のボーリング孔を利用して，18 点で地殻熱流量の測定を行った．また，新エネルギー開発機構 (NEDO) から3点のデータをいただき，それらのデータと今まで測定された結果と合わせて，中部日本の地殻熱流量コンターマップを作製した．この結果，以下のような特徴が明かになってきた．

1．関東中東部は低熱流量となっており，火山フロントに近付くにつれて，東北などの沈み込み帯にもみられるように，熱流量が急に高くなる．

2．東海地方西部も熱流量が低い．

これらはそれぞれ太平洋プレートとフィリピン海プレートの沈み込みの影響によるものと解釈できる．

地殻深部の熱的状態を調べるために，前の表面熱流量に基いて，二層（コンラッド面とモホ面）の地殻モデルを仮定して，モホ面の温度及びモホより下からくる熱流量，即ちマントル熱流量を計算した．

また，表面熱流量の分布をほかの地球物理の観測データと比較した結果，次のことがわかった．

1．深さ 16～47 km の地震波速度構造（石田，1987）と深さ 30～60 km の減衰構造（橋田，1987）は表面熱流量とほぼ対応している．つまり，表面熱流量が高いところでは，速度が遅くて，地震波の減衰が激しい．これらの一致はそれぞれの深さにおける速度構造と減衰構造が温度にかなりコントロールされていることを意味していると考えられる．

2．防災センターの関東-東海地震観測ネットワークで 1983～1985 年の間に記録されたすべての地震分布（石田，私信）と重ねてみると，東海地方東部の熱流量が高いところでは，深さ 40～60 km の間に，地震がほとんど起きてない．これは沈み込んだスラブが高温のため地震発生能力を失っているのではないかと推定される．

---

* 現在金沢大学理学部